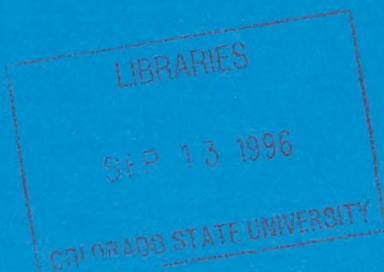


# **COMPARISON OF THE SIMULATED ARCTIC CLIMATE OF THE CSU GCM WITH OBSERVATIONS**

**by Cara-Lyn Lappen**

**David A. Randall, Principal Investigator**

**Colorado  
State  
University**



**DEPARTMENT OF  
ATMOSPHERIC SCIENCE**

**PAPER NO. 614**

# COMPARISON OF THE SIMULATED ARCTIC CLIMATE OF THE CSU GCM WITH OBSERVATIONS

by

Cara-Lyn Lappen

Research supported by the  
National Science Foundation  
under Grant number OPP-9504246  
and by the National Aeronautics & Space Administration  
under Grant number NAG1-1701

Department of Atmospheric Science  
Colorado State University  
Fort Collins, CO

July 1996

Atmospheric Science Paper No. 614



018401 3920536

DC  
852  
.C6  
no. 614  
ATMOS

## ACKNOWLEDGEMENTS

This work was supported by grant No. NAG1-1701 by the National Aeronautics and Space Administration and by grant No. OPP-9504246 by the National Science Foundation.

# Table of Contents

1.	Introduction.....	1
	1.1 Colorado State University General Circulation Model (CSU GCM).....	2
	1.2 Summary of Observations Used in Comparisons.....	3
	1.3 Methodology.....	3
2.	Standard Meteorological Parameters.....	5
	2.1 Temperature.....	5
	2.2 Winds.....	7
	2.3 Mean Sea Level Pressure.....	9
	2.4 500 mb Geopotential Height.....	9
3.	Cloud Parameters.....	13
	3.1 Low Cloud Fraction.....	13
	3.2 Middle Cloud Fraction.....	13
	3.3 High and Total Cloud Fraction.....	14
	3.4 Cloud Optical Depth.....	14
	3.5 Total Precipitation and Specific Humidity.....	16
	3.6 Summary.....	16
4.	Energy Budget.....	17
	4.1 Surface Albedo.....	18
	4.2 Net Short Wave.....	18
	4.3 Downward Long Wave.....	18
	4.4 Net Long Wave.....	19
	4.5 Latent Heat Flux.....	20
	4.6 Sensible Heat Flux.....	20
	4.7 Net Downward Energy Flux.....	21
	4.8 Surface Cloud Forcing.....	23
	4.9 Top-of-the-Atmosphere Radiation.....	23
	4.10 Summary.....	23
5.	Land Comparisons.....	24
	5.1 Albedo.....	25
	5.2 Clear-Sky Net Long Wave.....	25
	5.3 Downward Long Wave.....	25
	5.4 Net Long Wave.....	26
	5.5 Net Short Wave.....	26
	5.6 Net Surface Radiation.....	26
	5.7 Total Cloud Fraction.....	26
	5.8 Summary.....	27
6.	Summary and Conclusions.....	27
7.	Bibliography.....	30

# 1. Introduction

Arctic climate modeling plays an important role in our understanding of local Arctic climatic processes as well as the Arctic's role in global climatic processes. In the past, scientists have focused on middle and lower latitudes while they paid less attention to the polar regions. To fully understand the global behavior of the general circulations of the atmosphere and ocean, however, we need a detailed knowledge of Arctic processes and their interactions with global processes.

Understanding of Arctic climate poses some very tough challenges. We know little of the key climatic processes that occur in Arctic. This is a direct result of the lack of observational data. Much uncertainty leads to difficulties in parameterizing Arctic processes in climatic models. As a result, they are often parameterized crudely resulting in large discrepancies between simulated and observed climates, and among the climates simulated by different models. Such differences are associated with the varying representation of the state of the ocean-ice surface, and the interactions of cloud processes, atmospheric radiative transfer, surface energy components, and the planetary boundary layer with the changing surface state (Ebert and Curry, 1993).

To overcome some of these difficulties, we must understand the complex mechanisms that link the ice, atmosphere, and ocean. The key is a greater understanding of two important feedback mechanisms- the ice-albedo feedback and the cloud-radiation feedback (Moritz et al., 1993).

We understand the ice-albedo feedback mechanism as follows: As the temperature nears 0 °C, the highly reflective ice cover melts decreasing the total ice concentration. As this happens, more of the sun's energy is absorbed instead of reflected. Additional melting results from this enhanced energy input which further decreases the albedo, creating a positive feedback loop. In order to accurately represent the ice-albedo feedback in global circulation models, one must properly account for annual changes in ice thickness, surface albedo, snow/ice ablation and accretion, and their varying degrees of absorption of off-shore radiation (Moritz et al., 1993).

Cloud-radiation feedback is also an important mechanism. A perturbation to the surface energy balance results in changes in sea ice thickness, and thus changes in the surface albedo and surface temperature. This, in turn, alters the surface energy fluxes which cause changes in the temperature, pressure, and wind in the lower atmosphere. This induces changes to the cloud optical properties, which affect the surface energy balance closing the loop. For the cloud-radiation feedback mechanism, one must accurately represent the vertical and horizontal distribution of cloud cover, water vapor content, cloud particle concentration and size, and the changes that occur with atmospheric temperature and chemistry (Moritz et al., 1993).

The extensive ice cover of the Arctic Ocean allows the ocean to remain in a low-energy state, by reflecting away incoming solar energy. This contributes to the polar heat sink (Nakamura and Oort, 1988). In addition, ice formation affects the temperature and salinity balance of the ocean, providing a major driving influence in the global thermohaline circulation. These things must also be accurately represented before GCMs will be able to simulate Arctic climate and accurately represent the sensitivity of the global climate to perturbations in the Arctic system (Moritz et al., 1993).

In this paper, I examine the Colorado State University General Circulation Model's (CSU GCM) simulations of temperature, cloud cover, and radiation over the Arctic polar region and I compare these fields to available observational data. Then, I assess the model's ability to accurately represent Arctic processes and I pinpoint its deficiencies. This is critical if we hope to improve the accuracy of the simulation over the Arctic. I used GCM run #C145 which corresponds to the "CSU91" AMIP (Atmospheric Model Intercomparison Project)(Gates, 1992).

### 1.1 Colorado State University General Circulation Model (CSU GCM)

We use the CSU GCM to study climate primarily through research on clouds, the global hydrologic cycle, and land-surface processes. The model's prognostic variables include potential temperature, wind, mixing ratio of water vapor, PBL pressure thickness, turbulent kinetic energy, and ground temperature and moisture variables. It uses horizontal differencing based on a regular latitude-longitude grid with a resolution of 5 degrees in longitude and 4 degrees in latitude. One can set the number of vertical levels as a parameter.

The physical parameterizations include solar radiation, terrestrial radiation, the planetary boundary layer turbulence, cumulus convection, large scale precipitation, cloudiness, and land-surface processes. For more information see The Colorado State University General Circulation Model Users Guide (Randall et. al., 1995).

The prescribed boundary conditions of the GCM include realistic topography, and the observed climatological seasonally varying global distributions of sea surface temperature, sea ice thickness, surface albedo, surface roughness, and seasonally varying surface morphologies such as sea ice, land ice, ocean, and vegetation types. This immediately presents problems as many of these prescribed fields are poorly observed in the Arctic polar region.

As far as the Arctic is concerned, a couple of points are worthy to note here. In the GCM, surface (sea ice) albedo is a linear function of temperature. It ranges in value from 0.2 to 0.8 and is assigned a new value each day based on updated surface temperature. The ice is either there or not there; there is no fractional ice cover. If the ice is there, it is assigned a thickness of 1.0 meter- if not, 0.0 meters. The ice thickness is updated every month and it varies linearly over a month during which it is disappearing or forming. A value of 0.2m is assigned in transition months when the ice is melting and a value of 0.8 in transition months when the ice is growing. No meltponds or leads are allowed and the emissivity is one. No snow is allowed.

The model predicts sea ice temperature by calculating the temperature which occurs when the sum of the surface energy fluxes equals zero:

$$F_{SW} - F_{LW} - F_{SH} - F_C = 0.0 \quad (\text{EQ 1})$$

where  $F_{SW}$  is the flux of short wave energy at the surface,  $F_{LW}$  is the flux of long wave energy at the surface,  $F_C$  is the conductive flux into the ice, and  $F_{SH}$  and  $F_{LH}$  are defined as in Section 4.4 and 4.5.

## 1.2 Summary of Observations Used in Comparisons

As stated earlier, the observational data over the Arctic is sparse. This section briefly reviews the sources of the observations used in this paper.

Marshunova and Chernigovskii (1978) (MCRAD) compiled measurements of radiation values at specific locations in the Arctic. Scientists compiled the data from actinometric observations made in polar stations, drifting stations, and in expeditions. Other radiation sources cited include Curry and Ebert (1992); Huschke (1969); Vowinckel (1962); Marshunova (1961); Doronin (1963); and Maykut (1978,1982,1986).

Curry and Ebert (1992) calculated cloud optical properties from the Arctic Stratus Experiment and compiled radiation values from cloud observations made by Huschke (1969), Vowinckel (1962), and Gorshkov (1983).

Maykut, in all three sources, used sensible and latent heat data from Doronin (1963) who used the values from 26 years of drifting station temperature observations. They also all use shortwave and longwave values from Marshunova (1961) who obtained them from calculations using observed cloud distribution data as well as some surface radiation measurements from polar land and drifting stations. Maykut (1982) also used data from Arctic Ice Dynamics Joint Experiments (AIDJEX).

For cloud data, I used several sources. Although more data exists here than for other variables, the sources present a wide array of results. The large discrepancies between the observations originate partly from the bias of surface observations not to see high clouds and the bias of satellites not to see low clouds, and partly from errors in retrieval algorithms.

Warren et al. (1986) is a compilation from ship-based observations contained in the Comprehensive Ocean-Atmosphere Data Set (COADS). The C-matrix data set includes data from the NIMBUS-7 global cloud climatology from Show et al. (1988). One should use care when interpreting this data set, because the height classification schemes for low, middle, and high cloud fractions differ slightly from those used by the other sources and the GCM (see Section 3).

Other data used include analyses from the European Center for Medium-Range Weather Forecasts (ECMWF); the Coordinated Eastern Arctic Experiments (CEAREX) for comparisons of the modeled fields in the Greenland sea; National Center for Atmospheric Research (NCAR) precipitation data derived from Legates and Wilmont (1990); and some observations from AIDJEX.

## 1.3 Methodology

The CSU GCM represents the Arctic using a grid of 72x7 points. The model resolution is five degrees in longitude and four degrees in latitude. Latitude stretches from 60°N to the pole. The value at each point is for the center of the grid box. The row of boxes closest to the pole is six degrees "tall" in latitude stretching from 84 degrees to 90 degrees (Figure 1).

To do comparisons with other gridded data such as the ECMWF and the NCAR precipitation data, I interpolated values onto the GCM grid before comparison. I often use regional calculations in this paper to compare averages over large areas with those observed and calculated. I then area-weight the regional averages for each gridbox, to provide true averages.

For January and July, I compared monthly means in order to catch the extremes of winter and summer conditions. I averaged a minimum of four years (often more) for both the GCM and the observations.

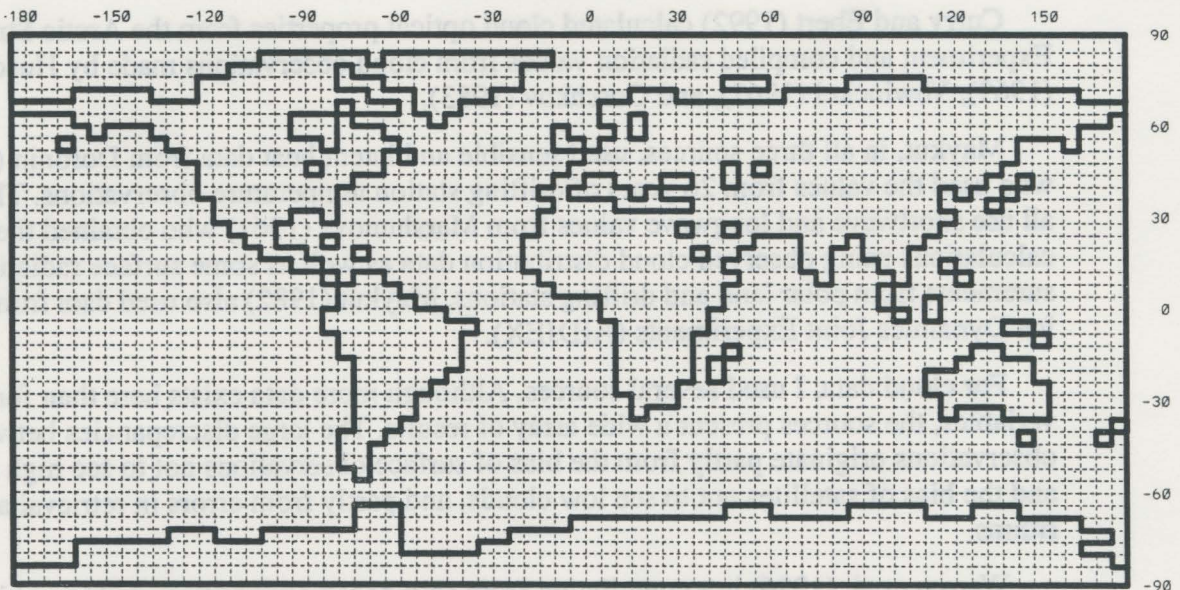


FIGURE 1 . The CSU GCM's grid

One set of comparisons divides the Arctic into four equal quadrants- the Greenland sea (GS) quadrant, the Kara/Norwegian Seas (KNS) quadrant, the Beaufort Sea (BS) quadrant, and the Laptev Sea (LS) quadrant (Figure 2). These comparisons use all points in each quadrant- land and sea. Another divides the Arctic into three regions to compare only points over water- the Greenland Sea, the Kara/Barent Seas (KBS), and the Arctic Ocean (AO). I also give total Arctic (TA) means with this comparison. Most of the comparisons are averages over oceans or seas.

The third set of comparisons is for individual points for land only, and uses a single value- the one corresponding to the GCM grid box which contains this point (Figure 2). Problems with unrepresentative points arise from doing these types of comparisons so I expect greater discrepancies in this section. (For example, the coarse GCM grid may not recognize a land point if it is an island or a thin peninsula). Thus, these results should only serve to give us indications of the overall performance of the GCM with respect to the examined variable- e.g., if the GCM consistently overpredicts or underpredicts values over an area.

In addition, I plotted vertical profiles of temperature and cloudiness for specific locations. I used these plots to try and explain some of the discrepancies identified in the comparison studies. For variables for which there are no observational data, I assessed the GCM values to determine if they are reasonable, given how they change over the Arctic and how well they correlate with variables for which we do have observations.

The data-comparison portion of this study is divided into four sections. The first includes comparisons of standard meteorological parameters such as wind, pressure, temperature (including soundings), and 500 mb geopotential height. The second examines cloud fields, including low, middle, high, and total cloud fractions as well as total precipitation, cloud optical depth, and specific humidity. The third gives radiation comparisons. It examines the surface energy components-net short wave (SW), net long wave (LW), net downward energy flux, sensible heat flux, latent heat flux, net surface flux, surface albedo, clear-sky net SW, clear-sky net LW, SW cloud forcing, LW cloud forcing, and total cloud forcing. It also includes discussions of the planetary albedo and net SW and LW at the top of the atmosphere. The final section discusses radiation variables measured at individual locations.

Following these comparisons, a summary and conclusions are presented, as well as suggestions for the changes needed to bring the model results into better agreement with the observations.

## 2. Standard Meteorological Parameters

Standard meteorological parameters include mean sea level pressure (MSLP), temperature, wind speed and direction, and the geopotential at 500 mb. The major source used for observations is the ECMWF analyses. However, data from Oort (1983) and Doronin (1963) were also used.

### 2.1 Temperature

The GCM has some problems with the surface temperatures for July. It consistently overpredicts them by about four degrees over oceanic regions. For January, the agreement is good except for the KBS region where it is seven degrees too cold (Table 1). I plotted temperature soundings from the ECMWF and the GCM and I compared them for several locations across the Arctic. The results show that the GCM predicts the surface temperature to be about four degrees too warm in July (Figure 3). A possible explanation is that the ice is too thin. A comparison of observed ice thicknesses over the region show that the ice thickness is greater than two meters where there is ice and where observations are available (Bourke and McLaren, 1992). The GCM sets the ice to one meter where it is present.

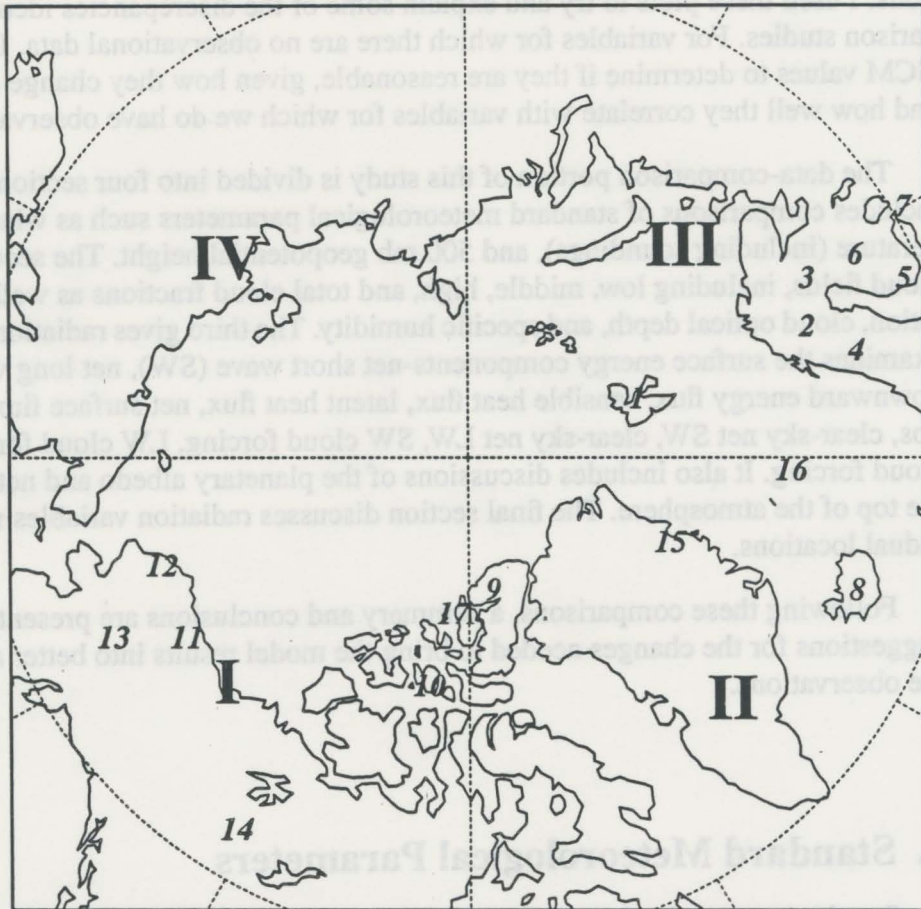


**FIGURE 2.** Roman numerals indicate the location of the four quadrants used in Table 4: I- Beaufort Sea Region; II- Greenland Region; III- Norwegian/Barent Region; IV- Laptev Sea Region. Alpha-numeric numbers indicate the location of the individual point measurements as follows: 1. Isfjord; 2. Tromso; 3. Karasjok; 4. Bude; 5. Kiruna; 6. Sodankyla; 7. Jokioynen; 8. Reykjavik; 9. Alert; 10. Resolute; 11. Inuvik; 12. Barrow; 13. Fairbanks; 14. Fort Simpson; 15. Myugbukhta; 16. Medvezhiv; 17. Eureka

In January, the underprediction of surface temperature by seven degrees in the KBS region may be a result of the error in the surface wind pattern (Figure 4). The observed surface wind in this region is from the south at approximately 5 m/s. These winds transport warm air from the south into the KBS region. The GCM has weak southerly or northerly winds in this region. Thus, the warmer southerly air is not advected over this region. This causes problems with the surface radiation components in this region as well (see Sections 4 and 5).

The GCM has a bias toward warm temperatures over land throughout the whole sounding. In July, over the Eurasian peninsula and over Canada, Greenland, and Alaska, the air temperature throughout the sounding is on the average about three to six degrees too warm (Figure 3). Over Canada and Alaska, this is true for January as well.

## 2.2 Winds

The GCM has a tendency to overpredict the magnitude of the surface horizontal wind speed. This effect is the most pronounced over the KBS region in January and mostly originates from the  $v$  wind (Table 1). In the previous section, I discussed the implications of this. Two major observed features of the Arctic wind pattern (based on drifting buoy data) are the Beaufort gyre and the Transpolar Drift Stream (TPDS). The Beaufort gyre encompasses the Beaufort Sea and pushes the ice in an anticyclonic pattern. The TPDS takes the ice from the Beaufort gyre and pushes it across the north pole through the Fram Strait east of Greenland. This is very important for the oceanic circulation as well as the surface radiative properties of the Arctic Ocean (Power and Mysak, 1992).

The GCM does a poor job in both months of capturing correctly the anticyclonic circulation in the Beaufort sea. In January, the simulated northerly winds, although extending from the pole to the Bering Strait, are significantly stronger than observed and interrupt the anticyclonic pattern (Figure 4). In July, the winds weaken considerably and I had difficulty discerning any circulation pattern (not shown). The GCM's inability to capture this feature undoubtedly has important effects on the radiative parameters I will discuss in Section four.

The GCM succeeds in predicting the wind direction, with three notable exceptions. One is the strong northerly winds discussed above near the Bering strait in January. A second is in the region of the Norwegian Sea in July, where the observed winds are southerly and the GCM's winds are northerly. Both of these regions show the largest differences in mean sea level pressure (MSLP)(discussed later).

The third region is the coast of Alaska in January. Over the Alaskan land mass, south-erlies associated with the Aleutian low are present in both the observations and the GCM. In the GCM, however, they are too strong and extend too far north (Figure 4). The north-erly winds flowing through the Bering Strait are also too strong. This leads to larger than observed convergence over the Alaskan coast. I will show later that this has a significant effect on the cloud and radiation fields in the area.

A comparison of vertical velocity fields was impossible. The ECMWF fields of vertical velocity show patterns consistent with the observed pressure and clouds fields, i.e., sinking over the pole and upward motion in the regions of the Davis Strait (west of Greenland), the Norwegian and Greenland Seas, and over the Bering Strait. The GCM vertical velocity fields over the arctic, however, were too noisy to interpret.



FIGURE 3. Temperature Soundings over Arctic Ocean and East Russia. Comparison between ECMWF and GCM.

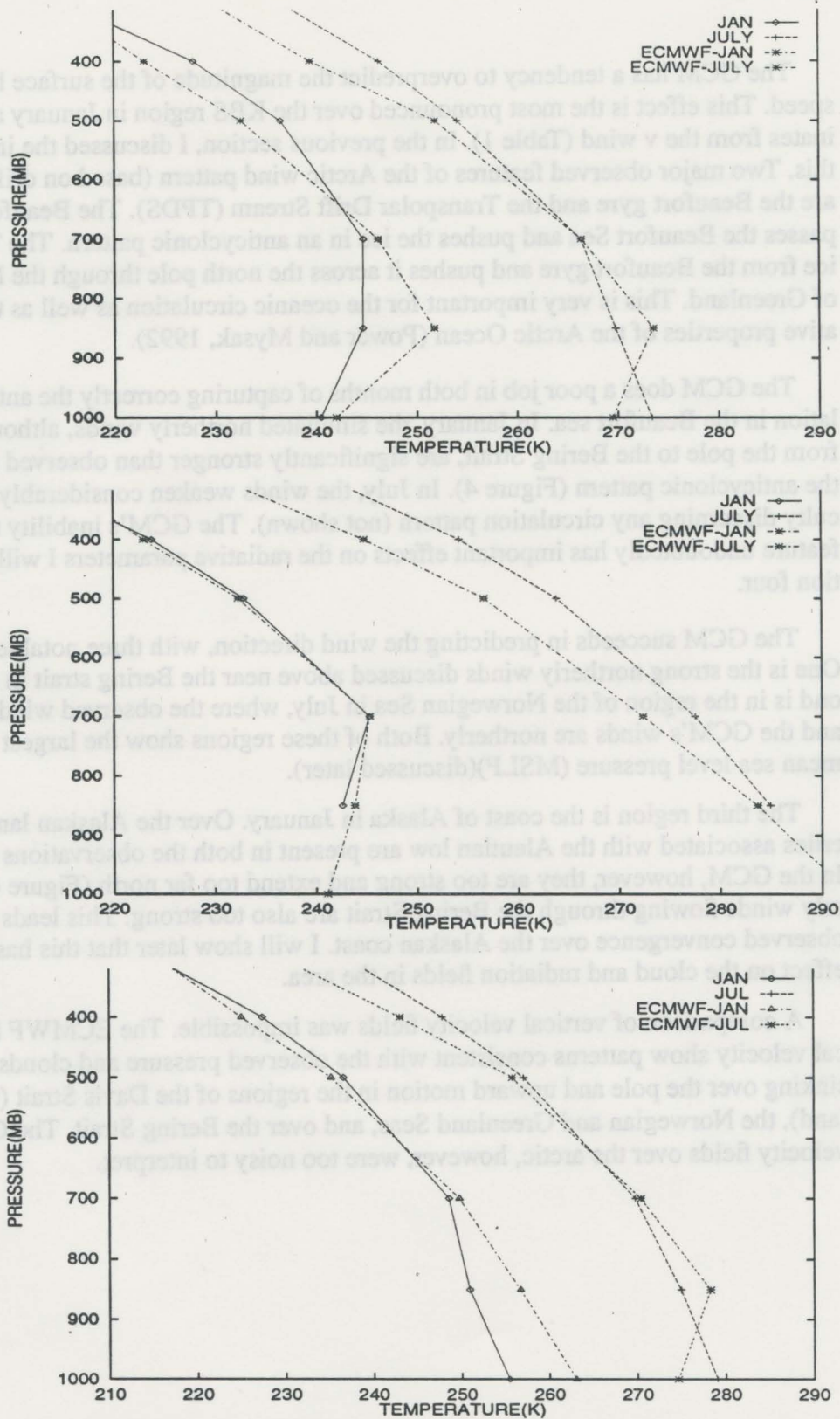


**FIGURE 3. Temperature Soundings over Arctic Ocean-top; East Russia mainland-middle; Barents Sea-bottom. Comparison between ECMWF and GCM**

## 2.3 Mean Sea Level Pressure

In general, the simulated and observed MSLP maps agree well for July. For January, however, the GCM grossly underpredicts surface pressure (Figure 5 a). In the Beaufort Sea region, this underprediction is as large as 24 mb. The relative pressures across the region agree well- both showing a relative high over the pole. Since the relative pressures agree well, the surface wind patterns are not significantly affected.

Since temperature is the driving force behind the surface pressure pattern, however, one would expect surface temperatures to be too cold over the region. While this is true over the Arctic Ocean, the Beaufort Sea surface air temperatures are a little too warm. The GCM's overprediction of the aerial extent of the Aleutian low may cause this.

One explanation for the low pressures across the Arctic is the specified smaller-than-observed ice thickness in the model in this region (see Section 2.1). This would cause warmer than normal surface temperatures and lower than normal surface pressures. Another less likely explanation is that the subsidence rate over the pole is too slow. Thus, even if the cooling rate is correct, the air cools for a longer period of time making the surface air too cold.

## 2.4 500 mb Geopotential Height

I compare the 500 mb geopotential heights with ECMWF data. The agreement is within 10 m for January. For July, the GCM has a high bias of approximately 100 m (Table 1). Two things could account for these excessive 500 mb geopotential heights. One is that the surface pressure is too high and the other is that the mean temperature of the column of air is too warm. A five degree temperature error or a 10 mb surface pressure difference could account for a ~100 m error in the 500 mb geopotential height. Simulated surface pressures in July are correct within a few millibars. Mean column temperatures are about 1 to 3 degrees too warm, which would account for approximately 50 m of the difference. The resulting error is about 50 m out of 5000 m, or about one percent. Integrating the hydrostatic equation could easily cause a 1% error with thick model layers.

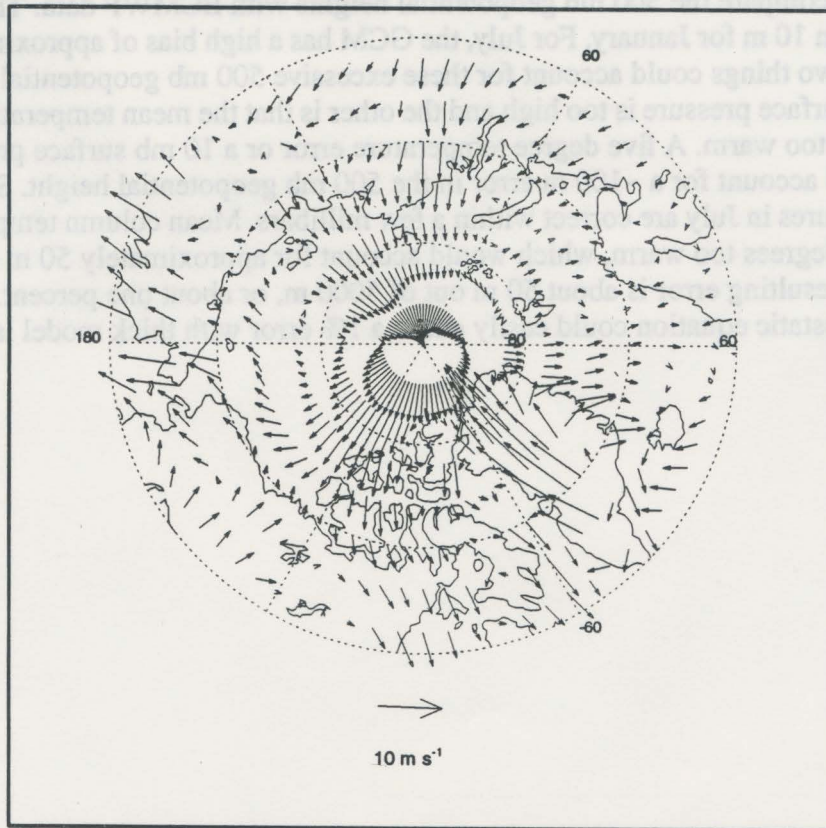
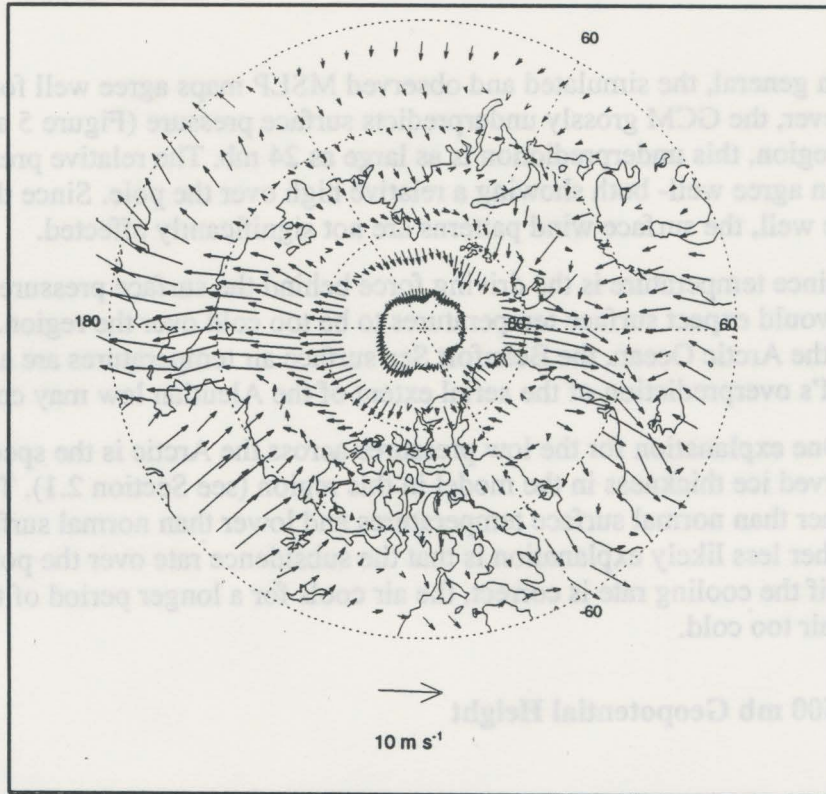


**FIGURE 4. January planetary boundary layer vector winds from the GCM- top and ECMWF- bottom**

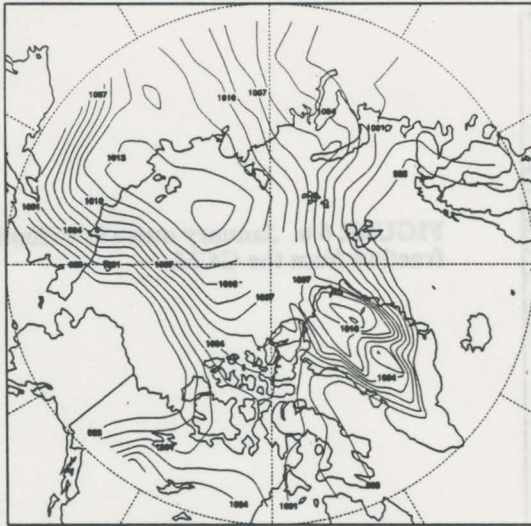


**FIGURE 5 a. January mean sea level pressure for the GCM, in millibars.**

**FIGURE 5 b. . January mean sea level pressure for the ECMWF, in millibars.**

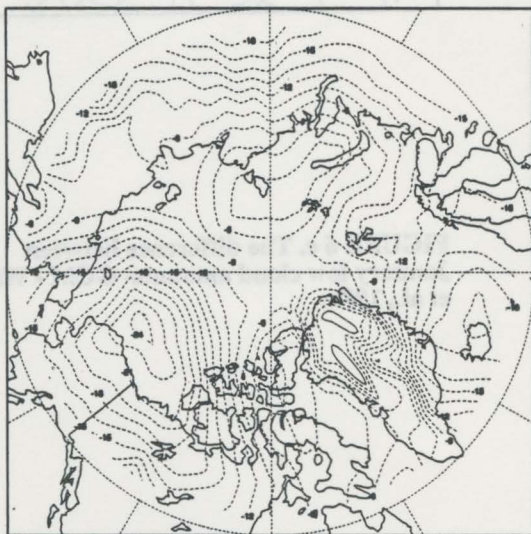
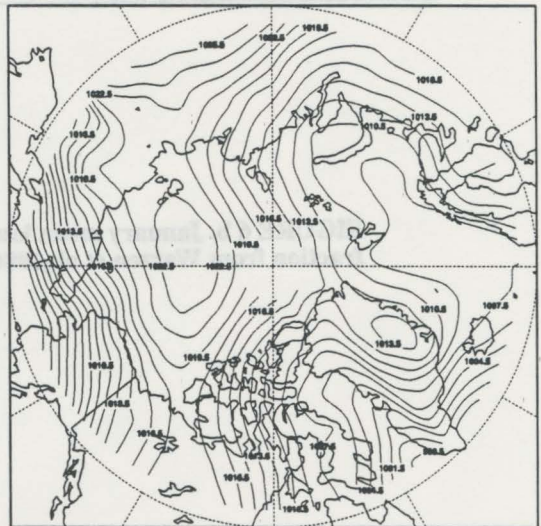


**FIGURE 5 c. . The difference between the January mean sea level pressures- GCM-ECMWF, in millibars.**

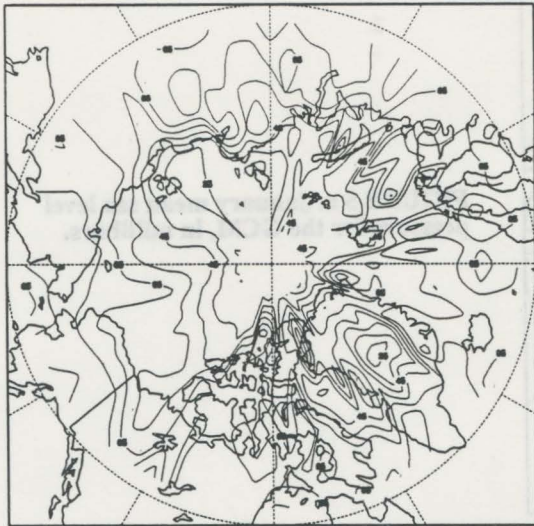


**FIGURE 6 a. January mean low cloud fraction from the GCM.**

**FIGURE 6 b. January mean low cloud fraction from Warren et al., 1986.**

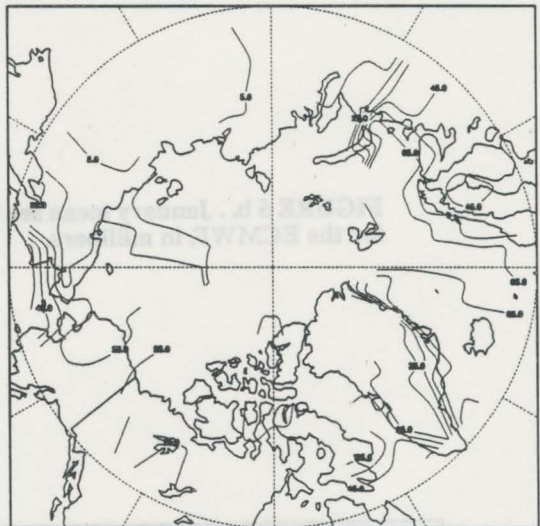


**FIGURE 6 c. The difference between January low cloud amounts- GCM - Warren et al., 1986.**

### 3. Cloud Parameters

Cloud parameters include cloud fraction as well as cloud optical depth, total precipitation, and specific humidity. Cloud fraction is defined as one minus the fraction of clear-sky. Three different categories divide cloud fraction- low cloud fraction, middle cloud fraction, and high cloud fraction. The levels defining these categories are the surface to 680 mb, 680 mb to 440 mb, and 440 mb upward, respectively. Low clouds consist of stratus, cumulus, stratocumulus, cumulonimbus, and fog. Middle clouds consist of altostratus, altocumulus, and nimbostratus. High clouds represent cirrus. I also investigate total cloudiness.

I used the observations of Warren et. al. (1986), Huschke (1969), Curry and Ebert (1992), and the NIMBUS-7 Global Cloud Climatology of Stowe et. al. (1988) (C-matrix) for comparison with the GCM for each of these three levels. I also compared the total cloud fractions. It is important to note here that Stowe et. al. define their cloud levels in a slightly different manner (low-sfc to 800 mb; mid-800 mb to 600 mb; high-above 600 mb). Thus, when using this data set for comparison, low and middle combined is the closest to the low classification of the others, and high represents approximately the levels covered by middle and high in the other sets.

Total precipitation includes rain and snow combined. I compare it with Vowinckel and Orvig (1970) and the NCAR precipitation data set compiled from Legates and Wilmont (1990). I compare specific humidity with Oort (1983).

#### 3.1 Low Cloud Fraction

In general, the GCM overpredicts low cloud amount over the ocean for January and severely underpredicts it for July (Table 2). Over land, the GCM overpredicts low cloud fraction for July (Figure 6 a). This brings the observed and predicted values closer for the total Arctic (land and sea). The one exception is the KBS region, where the GCM slightly underpredicts low cloud amount. The Stowe et. al. data are too low here as they define low cloud amount differently (as explained above). The very large errors in simulated low cloud amount in July manifest themselves in the radiation values that I examine in the next section. This is one of the key deficiencies in the CSU GCM's simulation of the Arctic climate. The warm northward flowing Norwegian current (which keeps the Greenland sea relatively warm all year favoring cloud formation) likely causes the large cloud cover (both simulated and observed) over the Greenland sea throughout the year. Another thing to note is that the cloud cover over Alaska is too high in January. The surface wind problem discussed in Section 2.2 causes this problem.

#### 3.2 Middle Cloud Fraction

For January, simulated middle cloud fractions exhibit close agreement with the observations (Table 2). If one adds the C-matrix middle clouds to the C-matrix low cloud fraction, the agreement is also good (see Section 3). For July, the GCM underpredicts cloud fraction in all of the individual sea regions. However, the mean for the total Arctic agrees with the observations. The model tends to overpredict middle cloud amount over land

areas and underpredict it over water (not shown). This explains the discrepancy. These two opposing effects result in the agreement of the mean for the Arctic as a whole. Combined with low cloud fraction, the GCM's underprediction of middle cloud fraction over ocean, for July, manifests itself in the surface energy components that I will discuss in Section four. As with low cloud cover over Alaska, the GCM overpredicts middle cloud fraction in January.

### 3.3 High and Total Cloud Fraction

Generally, the GCM overpredicts high cloud fraction. The agreement is worse in January than July (Table 2). Values in both months are close to those observed only for the AO region. For total cloud fraction, the results can be misleading as they represent the sum of the three layers. Often opposing errors balance out in the total to give an accurate estimate for an incorrect reason. The total cloud fraction does reflect major trends, however. For example, the GCM underpredicts total cloud fraction in July. This reflects the dominant influence of the underprediction of low and middle clouds, compared with the overprediction of high clouds. In the KBS region, however, the simulated total cloud fraction is close to that observed. Here, the change in low cloud balances an opposing change in high cloud, giving the right value for the wrong reason. The higher middle cloud fraction diagnosed over land masses (discussed in Section 3.2) causes the relatively large cloud cover (both simulated and observed) over the Greenland sea throughout the year.

Another misleading fact is the general agreement between the observations and the GCM over the Arctic Ocean for January. Examination of the AO region in this month shows that, over the Eastern AO, the cloud fraction is much lower than the observations, while over the Western AO, it is much higher (Figure 7a). An area average cancels out these errors and gives good agreement with the observed means.

Other observations of total cloud fraction can be seen in Table 2. Although this table is divided into quadrants which contain land as well as ocean, the results agree with the sea values indicating a general trend to underpredict cloud amount for July and to overpredict it for January

### 3.4 Cloud Optical Depth

In order to calculate cloud optical depth from the GCM, I identified the different types of clouds in a column, weighted each by an appropriate pressure thickness, and summed these thicknesses. I then assigned extinction coefficients for each cloud type. Thus, low clouds tend to be thicker and will contribute more to the total optical depth than higher clouds.

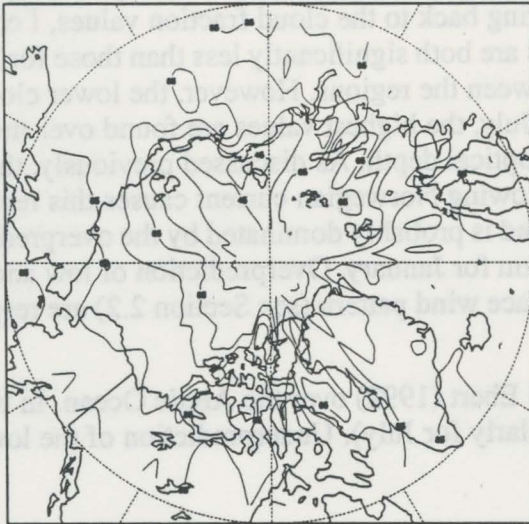


**FIGURE 7a. Mean total cloud fraction for the GCM in January.**

**FIGURE 7 b. Mean total cloud fraction from Warren et al., 1986 in January**

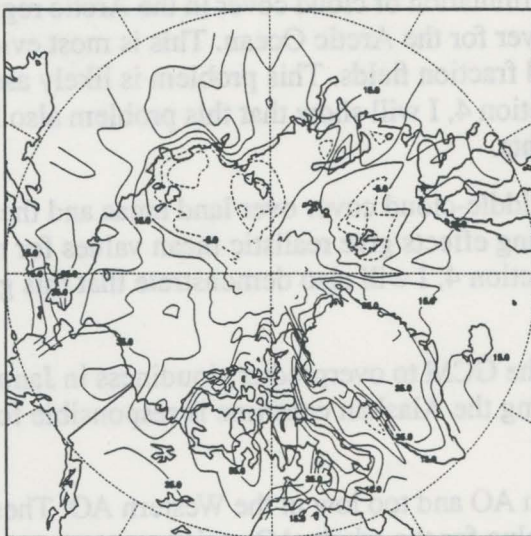
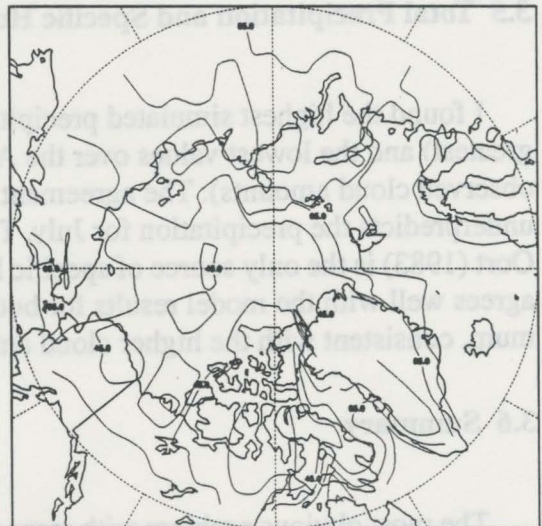


**FIGURE 7 c. Difference between the mean total cloud fractions- GCM - Warren et. al., 1986.**

The first thing to note about the GCM output is that the AO has a smaller optical depth than any other section (Table 2 and Figure 8). Referring back to the cloud fraction values, I can easily explain this. The low and middle cloud fractions are both significantly less than those for the other regions. High cloud fraction is less variable between the regions. However, the lower clouds contribute more to the optical depth. Similarly, for July, the highest values are found over the GS for low, middle, and high cloud fraction as well as optical depth. As discussed previously, the warm water influx to this region from the northward flowing Norwegian current causes this result. The highest value for January is for the total Arctic and is probably dominated by the overprediction of land clouds. Over Alaska, the value is a maximum for January. Overprediction of low and middle clouds, which results from anomalies in the surface wind pattern (see Section 2.2) are responsible for this discrepancy.

The only comparison here is with Curry and Ebert (1992) over the Arctic Ocean. In both seasons, the GCM underpredicts this value (particularly for July). Underprediction of the low and middle clouds directly cause this problem.

### 3.5 Total Precipitation and Specific Humidity

I found the highest simulated precipitation rates in the GS region (where cloud cover was the greatest) and the lowest values over the Arctic Ocean (where the GCM predicted lower than observed cloud amounts). The agreement with the observations is good for January, but the GCM underpredicts the precipitation for July. This is consistent with the underprediction of cloudiness. Oort (1983) is the only source of specific humidity data. It is data over the Arctic Ocean. This data agrees well with the model results for both months. Over Alaska, the precipitation shows a maximum, consistent with the higher cloud amounts (see sections 2.2 and 3.4).

### 3.6 Summary

The most obvious problem with respect to simulation of cloud cover in the Arctic region is the GCM's inability to simulate adequate cloud cover for the Arctic Ocean. This is most evident in the cloud optical depth fields and the low-cloud fraction fields. This problem is likely associated with an underprediction of precipitation. In Section 4, I will show that this problem also has a significant impact on the surface energy components.

Another problem is the overprediction of middle-cloud cover over land areas and the underprediction of it over the seas. These compensating effects give realistic mean values for middle-cloud fraction over the Arctic as a whole. In Section 4, I will also demonstrate that this gives correct results for incorrect reasons.

For Alaska, there is a definite tendency for the GCM to overpredict cloudiness in January. The overprediction of surface wind convergence along the Alaskan coastline is responsible for this overprediction.

Finally, cloud cover is too high in the eastern AO and too low in the Western AO. These errors balanced out to give a misleading good mean value for the whole AO region.

Although the GCM results and the observations differ greatly at times, the relative changes between regions generally show the correct trends. For example, the highest cloud amounts are found over the GS region in both the observations and the GCM.

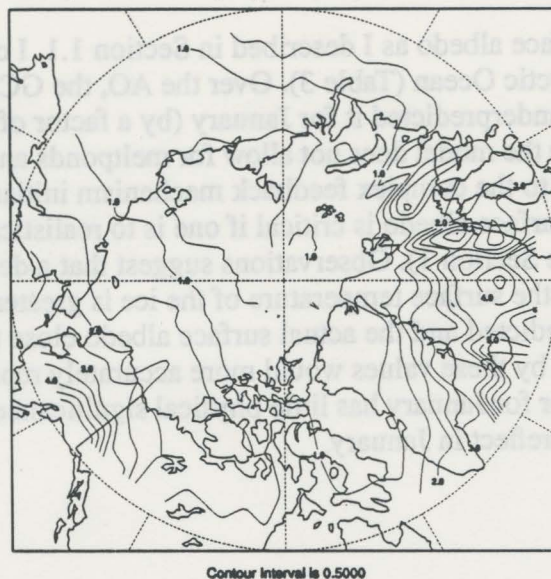


FIGURE 8. Mean cloud optical depth from the GCM in January

#### 4. Energy Budget

The components of the surface energy flux include surface net short wave ( $SW_{net}$ ), net long wave ( $LW_{net}$ ), downward LW, sensible heat flux (SH), latent heat flux (LH), net flux (which sums  $LW_{net}$ , SW, SH, and LH), SW, LW, and total cloud forcing, and albedo. I also compared some simulated top-of-the-atmosphere variables with observations. These include net SW, outgoing LW, and planetary albedo. I also examined clearsky net SW and LW at the surface despite that I found no observational data for comparison.

Longwave, SH, and LH are defined as positive upwards, while SW is defined as positive downward, so that positive net LW means that the surface is losing energy, while positive net SW means the surface is gaining energy.

I analyzed these for the oceanic sections defined in Figure two and listed in Table three, and for the four quadrants defined in Figure two and displayed in Table four. Table four also contains some additional comparisons for a region defined as all points north of 70°N.

The observations used for comparison with the model results include: Curry and Ebert (1992); Doronin (1963); Maykut (1978,1982,1986); Marshunova (1961); Levitt et al. (1978); Badgley (1966); Makshtas (1984); and some AIDJEX data.

#### 4.1 Surface Albedo

The model calculates surface albedo as I described in Section 1.1. I compared results only with values found over the Arctic Ocean (Table 3). Over the AO, the GCM overpredicted the albedo for July and severely underpredicted it for January (by a factor of two). For July, one expects a discrepancy because the model does not allow for meltponds and leads which reduce the surface albedo. However, due to the complex feedback mechanism initiated by surface albedo, accuracy in determining the surface albedo is critical if one is to realistically represent Arctic climatic processes in GCMs (see Section 1). Observations suggest that a decrease in the model surface albedo of 10 -20% when the surface temperature of the ice is greater than 0°C would be enough to bring the model-predicted and the actual surface albedo close to agreement. Thus, the feedback mechanism initiated by these values would more accurately represent those in the observations. The factor of two error for January has little physical significance since there is very little incident short wave energy to reflect in January.

#### 4.2 Net Short Wave

The net surface SW depends on surface albedo and cloud cover (the higher the albedo and the higher the cloud cover, the lower the net short wave). The net SW varies in July across the Arctic (Table 3). These variations are systematic and are in accord with what one would expect. In the GS, where the sea is ice-free year round, low surface albedos and a higher net SW would be expected and are observed. The only comparison with the observations that we have been able to make is for the Arctic Ocean region, for which the agreement is good. This agreement is misleading, however. In the previous section, I showed that the surface albedo is too high over the Arctic Ocean. One would thus expect the net SW to be too low. The lower-than-observed simulated cloud cover in July over the Arctic Ocean (see Section 3) allows more total solar energy to reach the earth's surface, offsetting the effect of the excessive albedo. Thus, the GCM gives a correct value for the net surface SW for incorrect reasons.

#### 4.3 Downward Long Wave

The downward long wave radiation at the surface is directly affected by three variables- the mean temperature and water vapor content of the air, and cloud cover. As I showed previously, the GCM tends to underpredict cloud cover in July- especially over the Arctic Ocean- and overpredicts it in January. Two exceptions are the GS region and the eastern Arctic Ocean (Section 3.3). This should bias the downward long wave to be lower in July and higher in January over the appropriate regions.

The GCM shows an increase in the downward long wave flux from January to July, which is to be expected from the higher temperatures and higher cloud amounts (Table 3). The lowest overall values for the regions studied are for the Arctic Ocean for both months. The underprediction of

clouds there in July and the colder mean temperatures in January (Section 2.1) undoubtedly cause this discrepancy. Another interesting thing to note is that for July, the total Arctic mean is larger than the values for any of the individual oceanic regions. This is a result of the GCM's overprediction of middle and low clouds over land, as discussed in Section three.

Large differences are observed over the region as a whole. The difference between the AO and the GS is more than  $95 \text{ Wm}^{-2}$  in January. It can be explained by the fact that the atmosphere is warmer over the GS than the AO by more almost twenty degrees (not shown). This could account for  $\sim 70 \text{ Wm}^{-2}$ . In addition, the GCM shows almost 5 times as many clouds over the GS region than over the Arctic Ocean. This factor acts to further increase that number (Table 2). The numbers thus make sense from the GCM standpoint.

Over Alaska (not shown) in January, downward longwave is a maximum. While there are no measurements of this quantity for Alaska, the simulation is consistent with the cloudiness results discussed earlier, which showed higher cloud coverage in this region (see Sections 3.1 and 3.2).

When compared with observations over the Arctic Ocean, however, there is some disparity. For July and January, the GCM underpredicts the downward longwave radiation over the Arctic Ocean. For July, one can easily explain the differences by the underprediction of clouds. For this month, the ECMWF and the GCM temperature soundings show approximately equal mean temperatures. Thus, temperature errors cause little or none of the downward longwave error. For January, the discrepancy is only  $15\text{-}20 \text{ Wm}^{-2}$ . This report shows cloud fractions to be close overall, as is the mean temperature of the atmosphere. It is difficult to say why the GCM is slightly lower here. However, the differences are small and they are within the range of observational errors.

#### 4.4 Net Long Wave

The net LW is defined as  $\text{LW}\uparrow - \text{LW}\downarrow$ . Positive means the surface is losing energy. In general, the values do not vary much across the Arctic. Since I showed  $\text{LW}\downarrow$  to vary greatly over the region in January, there must be a compensating effect in the  $\text{LW}\uparrow$  term. Long wave up is affected solely by the temperature of the ground since we assume that the surface emittance is one. For example, one would expect that the surface temperature over the GS will be higher than that over the Arctic Ocean in order to compensate for the large difference in the  $\text{LW}\downarrow$  (Section 4.3). Table one shows this to be true- the difference is 25 K.

The comparison with observations over the Arctic Ocean shows that the GCM overpredicts net LW for both months. The surface is cooling too much. This cooling is very large in July. This either means that the surface temperature is too warm, the atmospheric temperature is too cold, or there are not enough clouds. As shown in Section three, the model underpredicts cloud cover over the Arctic Ocean. With no clouds to trap the outgoing LW, the surface "should" have a large anomalous cooling. In January, a combination of factors are contributing to the error. Over the Arctic Ocean, the air temperature is too cold and the surface temperature is too warm (Table 1). Both these factors also contribute to the July anomaly.

For Alaska, the net long wave is very low (not shown). This is due to the maximum in downward long wave (Section 4.3).

#### 4.5 Latent Heat Flux

For saturated surfaces like ocean and ice, the latent heat flux (LH) is parameterized in the model as a function of the difference between the saturation mixing ratio at the surface and the vapor mixing ratio of the atmosphere. It is proportional to the rate of evaporation from the surface. Since evaporation takes energy from the ground and puts it into the atmosphere, LH is positive upwards when evaporation is occurring. Two factors affect evaporation- the humidity difference discussed above and the wind speed near the surface:

$$LH = \rho L_v |V| C_T \{q^* - q_A\} \quad , \quad (EQ 2)$$

where  $\rho$  = air density,  $L_v$  = latent heat of vaporization,  $V$  = surface wind speed vector,  $C_T$  = the transfer coefficient,  $q^*$  = saturation mixing ratio at the surface, and  $q_A$  = vapor mixing ratio.

The data used for comparisons in this section come from a variety of sources (See Table 3).

As shown in Tables three and four, the model results agree well with observations with one notable exception. Over the GS region in January, the model shows a  $55 \text{ Wm}^{-2}$  latent heat flux. The observations show this to be near zero. In January, the model humidity difference between the water and the atmosphere (not shown) is an order of magnitude higher than for any other region examined. The magnitude of the latter causes this large difference. The overprediction of clouds in the GS (see Section 3) may be a result of anomalously high atmospheric mixing ratios. In addition, wind speeds in this area are a factor of two higher than in the other regions of the Arctic. Thus, one would expect the latent heat fluxes to be higher.

The observations do not show this, however. One can explain this by the difference in the surface wind pattern (Figure 4). Surface winds are four times larger in the GCM than in the observations. In the observations, wind speeds are near zero. In addition, as I discussed in Section 2.1, the surface observed winds are from the south. Thus, they advect warmer, moister air over the region reducing the difference between the saturation vapor pressure and the vapor pressure of the air above the ground. This reduces the latent heat flux.

#### 4.6 Sensible Heat Flux

The difference in temperature between the surface and the atmosphere parameterize the surface sensible heat flux (SH). I define it as positive upwards:

$$SH = \rho C_p C_T |V| (T_S - T_A) \quad , \quad (EQ 3)$$

where,  $\rho$  = air density,  $C_p$  = specific heat constant,  $C_T$  = the transfer coefficient,  $V$  = surface wind speed vector,  $T_S$  = surface temperature, and  $T_A$  = air temperature.

In January, tables three and four show that the surface sensible heat flux is positive in the GS and KBS regions and negative across the rest of the Arctic. The difference in temperature (ground minus surface) is greater than 5 K for both the Greenland Sea and the Barents Sea (BAS) (Figure 9). The KBS region, however, also includes the Kara Sea where this temperature differ-

ence is -1K. This mediates the affect on the average flux over the KBS region, making the value there smaller than in the GS region.

I derive all the data used for comparisons in this section from a variety of sources (see Table 3). One should keep in mind, however, that observing SH is difficult. Thus, the values may not be accurate. When comparing the January simulation with the observations, one sees that the sign of the result agrees in all cases. The magnitude over the AO is good, but in the GS it is double the observed value. The surface temperatures, which are slightly colder than observed (~2 K), partially cause this problem. In addition, wind speeds in the model, which are a little high, enhance this effect.

For the Beaufort Sea (BES) in January and for the in GS in July, the sensible heat flux is too strongly downward. Both higher than observed wind speeds and warmer than observed temperatures in both areas likely contribute to this discrepancy.

The July fluxes are negative, indicating that the surface air is warmer than the ice. For the ice and ocean, one expects this. I noted one interesting point-- although the fluxes in individual regions are negative, the average flux over the total Arctic is positive. Over land, in July, the sensible heat fluxes are strongly positive. The strong heating of the land in the summer causes this heat flux. Thus, the land fluxes dominate the ocean fluxes when averaged over the whole Arctic. This creates a net positive for July.

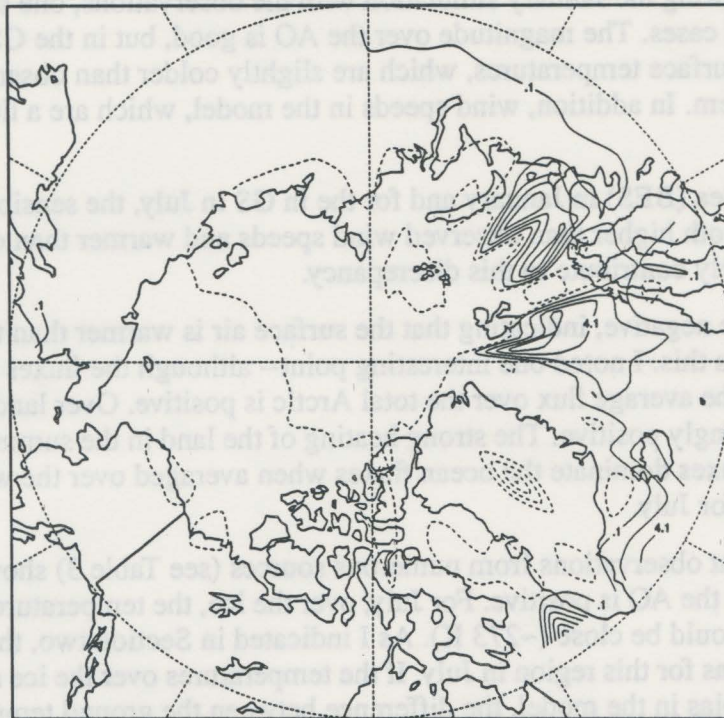
One problem is that observations from numerous sources (see Table 3) show that the surface sensible heat flux over the AO is positive. For July, over the ice, the temperature of the ice surface and the atmosphere should be close (~273 K). As I indicated in Section two, the GCM has a four to five degree warm bias for this region in July. If the temperatures over the ice are close and there is a warm surface air bias in the model, the difference between the ground temperature in the model and the air temperature in the model will be negative. Although the observations show that the flux is positive, the value is small (less than  $5 \text{ W m}^{-2}$ ). This indicates that the temperatures are in fact close. Melt ponds and leads which absorb more solar radiation and make the surface temperature slightly warmer than the surface air temperature cause this difference to be slightly positive.

#### 4.7 Net Downward Energy Flux

The net downward heat flux at the surface is the sum of the radiative and turbulent heat fluxes.  $SW_{\text{net}} - LW_{\text{net}} - LH - SH$  is the formula for calculation of the flux. For the Arctic Ocean, the downward heat fluxes are close to the observations in January, but are a little low in July. The component fluxes in this area match the observations well for January as I discussed in Sections 4.2, 4.4, 4.5, and 4.6. For July, however, the individual fluxes do not agree well.

The July net SW was in agreement for the wrong reason (Section 4.2). The sensible heat flux was negative in the simulations and positive in the observations. In addition, the net LW was a little high. Both of these contribute to the low values of net downward heat flux in July. However, due to the net SW problem, this GCM result may also be close to observations for an incorrect reason

In Table four, it can be seen that the Beaufort Sea region and the region defined as north of 70°N both show good agreement for both months. I found no components for these regions and thus cannot say whether these values are accurate due to compensating errors.



Contour Interval is 2.000

**FIGURE 9.** The difference between the ground temperature and the surface air temperature from the GCM in January.

Over the Greenland Sea, there is a definite problem for both months. The net surface energy flux in January and July is too strong upwards and downwards respectively. It is difficult for me to say why this is the case. The only GS data available for comparison are the turbulent fluxes. For January, the latent and sensible heat fluxes can account for most of the difference. For July, the sensible and latent heat flux differences approximately offset each other (Table 4). A combination of the differences in the SW and LW net fluxes must cause the large value of net surface energy flux that the GCM predicts. While there are no direct GS measurements of these, we can deduce a value from comparing the cloud and temperature fields.

As discussed earlier, the GCM underpredicts the cloud amounts and overpredicts the surface temperatures in July. Both of these contribute to a larger than observed  $LW_{net}$ , giving rise to an insufficient net downward heat flux. Thus, the difference in the SW absorbed must be the predominant contributor. It must be significantly larger than the observations. The low cloud amount as well as the low values of model's surface albedo will also contribute to this.(Section 4.2).

## 4.8 Surface Cloud Forcing

Cloud forcing is a direct measure of the difference in the radiation fields between clear-sky and all-sky conditions. In Section four, I analyzed the all-sky conditions. I will thus mention the GCM results for the clear-sky, although no data is available for comparison. The clear-sky short wave is affected by the planetary albedo and the surface albedo, and the clear-sky net long-wave by the surface and mean air temperatures. July clear-sky net SW in the GCM is lowest over the AO, and the clear-sky net LW is fairly uniform across the Arctic. The surface albedo is higher than observed by ~10-20%(Table 3). This results in the SW difference over the AO.

The simulated total (SW and LW combined) cloud forcing is realistic when one compares them to observations over the Arctic Ocean (Curry and Ebert(1992)). Opposing effects for the short-wave and long-wave components, however, cause the results to be misleading for July. The shortwave cloud forcing is too weak ( $22 \text{ Wm}^{-2}$  versus  $-100 \text{ Wm}^{-2}$ ) and the long wave cloud forcing is too small ( $13 \text{ Wm}^{-2}$  versus  $80 \text{ Wm}^{-2}$ ). The underprediction of clouds in July likely causes both discrepancies, and explains why the values over the Arctic Ocean are in general smaller than for the other regions examined. The fact that cloud forcing over the total Arctic is greater than for any of the individual oceanic regions is an interesting point to note. The model's overprediction of cloud cover over land discussed in Section 3.2 causes this.

## 4.9 Top-of-the-Atmosphere Radiation

I examined the following two top-of-the-atmosphere parameters: net SW radiation and outgoing LW radiation (OLR). In general, the GCM predicts the OLR at the top to be fairly uniform across the region within each month. The net short wave shows some variability, with the lowest value over the Arctic Ocean. This is consistent with the fact that the planetary albedo is largest in this region.

The only observation available to compare with these model results is the region north of  $70^{\circ}\text{N}$ . Over this area, the planetary albedo and the outgoing long wave are within 8% of the observed values for both January and July (Table 4). The net short wave, however is too high by approximately  $40 \text{ Wm}^{-2}$ . This is due to the lack of clouds in the model. Clouds act to reflect the incoming solar radiation making the net at the top of the atmosphere smaller. The underprediction of clouds means that less short wave is reflected back to space. This makes the absorbed SW too high.

## 4.10 Summary

The energy flux directly depends on many of the variables that I already discussed in Sections two and three. Thus, this section showed how many of the errors cited in the previous two sections combined to affect radiative forcing. In other words, I have explained the energy flux discrepancies of Section four as combinations of errors in clouds, temperature, and wind.

The GCM's underprediction of clouds over the AO in July causes a majority of the problems in the radiation simulations. Due to this one error, the GCM underpredicts the  $\text{LW}\downarrow$ , overpredicts

the  $LW_{net}$ . These cause the net downward heat flux to be too low, cloud forcing too weak, and the  $SW_{net}$  at the top of the atmosphere too large. This does not affect the  $SW_{net}$  at the surface due to a compensating error in the surface albedo (see Section 4.1).

Other less serious problems stemmed from the overprediction of land clouds in July, the four degree warm bias of surface temperatures in July across the region, the colder atmospheric temperatures over the Arctic ocean in January, and errors in the surface winds in the GS and along the Alaskan coast.

The GCM correctly captures the relative changes between January and July for most cases, but large errors existed in the actual value of the variable. For example, I showed that the downward long wave increases from January to July, but the GCM underpredicted both when compared with observations. As a result, the model overpredicted in both months the net long wave.

Incorrect surface winds, which advect and act to increase the temperature difference between the land and the sea, cause erroneous simulated latent and sensible heat fluxes in the GS in January. These factors combined to make the net downward heat flux too strong. In July, I deduced that the error in downward heat flux over the GS is a problem related to the  $SW_{net}$ . In addition, I showed the warm bias in July made the sensible heat flux there negative. In the observations, it is weakly positive.

Errors in the cloud fields effected the short wave and long wave cloud forcing in opposite senses. This made the total cloud forcing agree with the observations. Excessive net (absorbed) short wave radiation at the top of the atmosphere were also caused by cloud deficits.

Often, the sign of a variable averaged over the whole Arctic basin is opposite to the sign for the individual regions studied. Inclusion of land points (for which opposing errors were often found- for example, sensible heat flux) often caused this to occur.

Finally, I noticed radiation anomalies over Alaska caused by GCM overprediction of clouds in this region. This induces the model to diagnose a value for the downward LW which is too high and one for the net SW which is too low.

## 5. Land Comparisons

The comparisons done in the previous sections focused mainly on oceanic regions. In this section, I compare various measurements from land stations with the GCM results. I performed no averaging. The GCM point chosen for comparison was the grid box which encompassed the point where instruments made the surface observation. Undoubtedly, discrepancies will arise from points which are unrepresentative of the grid box in which they occur. Thus, the results of this section are meant to serve merely as corroboration for results of Section four, or to note trends over a region. Figure two shows the location of these points. Marshunova and Chernigovskii (1978) is the source of the observations. Table five displays the results.

## 5.1 Albedo

I compared only three locations due to data availability. For Sodankyla and Jokioynen (over Scandinavia) the GCM has a higher-than-observed albedo and for Resolute, a lower-than-observed albedo. The GCM shows that Resolute is completely snow covered in July. This fact may be responsible for the difference there. Difference occurs over the other two points. Perhaps, the simulated Scandinavian snow cover is too low.

## 5.2 Clear-Sky Net Long Wave

The overall results for the clear-sky net longwave show that the GCM is a little high in both January ( $\sim 10\text{-}20 \text{ Wm}^2$ ) and July ( $\sim 20\text{-}30 \text{ Wm}^2$ ). This must be due to a ground temperature which is too warm or a mean air temperature which is too cold. For most of these points, the surface temperature is too warm in January. One place stands out here as having larger than normal discrepancies- Reykjavik in January. The explanation for Reykjavik relates to the model's coarse resolution. Iceland is too small to be recognized as land by a GCM gridbox. Thus, the model thinks this location is a relatively warm ocean point. Its upward LW flux is thus anomalously large. In July, surface temperatures across the Arctic are 4-5 K too warm. At 275 K, a five degree temperature bias can account for a  $22 \text{ Wm}^2$  difference in the long wave radiation- almost exactly what the surface energy balance needs. One exception is over northwest Canada where the surface temperatures are slightly colder than observed. This is consistent with the fact that the GCM has a value which is too low over Inuvik.

## 5.3 Downward Long Wave

In general, the downward longwave in the GCM is too weak for both months. The exceptions are Inuvik, Barrow, and Fairbanks in January. As discussed in previous sections, over the Alaskan peninsula in January, the model overpredicts cloud amount as a result of the surface winds showing higher than observed convergence there. Thus, one would expect anomalously high downward heat fluxes in this region.

Downward long wave is a function of cloud amount and the mean air temperature. For the points considered here, except Alaska, the simulated mean air temperature is too cold (Figure 3) in January. This is the major contributing factor to the error in the downward longwave since cloud amounts are either close or slightly higher than observed. The error over Isfjord is larger than the rest and represents an anomalous area of cloud underprediction in January. This enhances the differences due to temperature (Figure 7a)

For July, the weaker than observed simulated downward longwave is due to the underprediction of cloudiness (Section 3). The areas with large underpredictions of downward longwave correspond to the areas with the largest cloud anomalies (for example-Isfjord)

## 5.4 Net Long Wave

The simulated net surface LW is low for Alaska and high everywhere else in January. It is high everywhere in July. This means that the surface cools too much. I explained in the previous section why the GCM is low for Alaska. The last section also provides a simple explanation for the fact that the GCM is low everywhere else -  $LW_{\downarrow}$  is too high.

Two locations have unusually high values, however, and these do not correspond to unusually low values of  $LW_{\downarrow}$ - Isfjord and Resolute. A likely explanation is that these two points are islands and the GCM cannot resolve them. The GCM grid boxes used to represent both of these stations are ocean points (Figure 1). Thus, the root of the large discrepancy comes from the  $LW_{\uparrow}$  term, which is governed by the surface temperature for which large differences exist between land and ocean.

## 5.5 Net Short Wave

For all the points examined, the GCM's net surface short wave is too low, with two exceptions- Isfjord and Reykjavik. The underprediction is worst over Canada and Alaska. I discussed in section three that the GCM severely underpredicts clouds over the Arctic ocean and overpredicts them over land- the worst overprediction being the Alaska and Northern Canada area. This explains why these land points all show a net radiation at the surface which is too low and why the worst values are over Alaska- clouds act to reflect the incoming solar energy.

As far as the two anomalous points are concerned, the GCM once again "thinks" they are ocean points- not land. The ocean has a lower surface albedo and absorbs more solar radiation. In Isfjord, there is an additional effect- the GCM underpredicts low and middle clouds in the GS (Section 3).

## 5.6 Net Surface Radiation

It is difficult to diagnose the net surface energy flux due to the fact that only radiative fluxes are available for comparison at these locations. In January, the GCM captures the correct sign of the net radiation flux and the magnitudes are fairly close. In July, however, the GCM severely underpredicts the magnitude of the net radiation flux for the three points examined. The  $LW_{\text{net}}$  is too high by about  $20 \text{ Wm}^{-2}$  and the  $SW_{\text{net}}$  is too low by  $\sim 50\text{-}60 \text{ Wm}^{-2}$ . This combines to account for most of the difference. Sensible and latent heat fluxes together account for the remainder.

## 5.7 Total Cloud Fraction

For January, the GCM overpredicts clouds everywhere. For July the results are more variable, but in general, the points in the GS region- Isfjord, Reykjavik, and Medvezhiv- all have cloud fractions which are lower than observed and the points in the Alaska region- Fort Simpson, Bar-

row, Fairbanks- all have higher than observed cloud fractions (see Section 5.5). This supports the results of Section three.

## 5.8 Summary

The results of this section show that the land points studied are consistent with the results of Section four. They indicate the following trends: The GCM overpredicts surface albedo, underpredicts downward long wave and net short wave for both months, and overpredicts net long wave and cloud fraction for both months. The excessive cloud cover for Alaska discussed in section three (and confirmed in this section) is the only exception.

## 6. Summary and Conclusions

The climatic processes of the Arctic have far reaching implications for the climate of the whole globe. It is also clear that due to the relatively low availability of Arctic observations, we poorly understand Arctic processes. A major tool which helps us understand global climatic changes is the General Circulation Model. Errors in the GCM fields of Arctic cloud formation, radiative properties of sea ice, and wind flow patterns combine to manifest themselves not only as errors in the simulated Arctic climate, but also as simulated global climatic errors. Until these processes are better understood, we cannot improve the models.

This purpose of this paper is identification of areas where major problem occur in the simulation of the Arctic climate by the Colorado State University General Circulation Model. I accomplish this by comparing the results of the GCM with available observations. I hope that by identifying the shortcomings of the CSU GCM over the Arctic, I provided a focus for future changes to the model. These changes, once enacted, should provide not only a more realistic Arctic climate, but a more realistic global climate as well.

For this analysis, I examined monthly means for January and July for variables separated into three categories- Standard Meteorological parameters, cloud variables, and radiation variables. I separated these categories further for regional comparisons. The regions are listed in tables one through four. The results pinpointed not only the regions of largest errors, but the large differences between the processes that occur over Arctic land masses and adjacent seas.

I traced most of the errors to five standard parameters- temperature, pressure, winds, clouds, and albedo. I found that these problems were often directly related to sea ice thickness which is represented crudely in the model as either 1m or 0 m for each gridbox (Section 1.1). The actual sea ice distribution in the Arctic varies greatly. This variation causes a surface temperature distribution, which causes a surface pressure distribution which in turn dictates the surface winds. Thus, errors in the ice thickness can help to explain many of the errors in these five standard parameters. This in turn leads to the errors found in the cloud and radiation fields.

One can summarize the basic errors associated with the five standard parameters as follows:

1. The temperatures over the entire Arctic in July are too warm. They agree in January except for the KBS region where they are too cold.

2. The GCM slightly overpredicts average wind speed for the four regions defined in figure two, independent of month.
3. Simulated wind directions agree well with the observations with three notable exceptions- the Bering strait in January, the Norwegian Sea in July, and the Alaskan peninsula in January. The large variability in observed sea ice thickness distributions as compared with the uniform value of 1m assigned by the GCM cause this difference.
4. Simulated mean sea level pressure is low by 10-20 mb across the Arctic in January, although the model captures relative changes in pressure.
5. The GCM overpredicts geopotential height in July by 100 m. One can explain half of this error by the mean column temperatures which are 1-3 degrees too warm in the model.
6. The GCM underpredicts low and middle clouds over the AO in July and overpredicts them in January. Over land, the model overpredicts low cloud fraction in July. Thus, in July, these effects balance and give a total Arctic cloudiness value which is close to the observed value.
7. The GCM tends to overpredict high clouds over the region with the exception of the AO where the simulated high cloudiness agrees well with observations. This agreement in the AO is misleading. It is the sum of two opposing errors- the underprediction in the eastern AO and the overprediction in the western AO.
8. The model overpredicts surface albedo over the AO in July. Melt ponds which are not recognized by the GCM undoubtedly affect this. A decrease in the model surface albedo of 10-20% should bring the model and the observations close to agreement.

These basic errors were the roots of problems in the radiation fields at the surface and at the top of the atmosphere.

I found that, often times, radiative parameters that were affected by more than one of the listed basic errors, but they offset one another, giving results which were close to the observed values. An example of this is the net surface short wave. A larger than observed surface albedo reduced it, and the underprediction of clouds increased it. This gave an overall value which was close to that observed.

The basic errors combined to effect the surface energy budget in the following ways.

1. The simulated net short wave is as described above. Offsetting errors, which were reduced by the larger-than-observed surface albedo and increased by the underprediction of clouds, affect it. They give an overall net SW which is close to that observed.
2. The simulated LW $\downarrow$  is too low over oceanic points and too high over land giving an overall Arctic mean that is close to the observed.
3. A combination of the underprediction of LW $\downarrow$  and the underprediction of LW $\uparrow$  cause the simulated LW $_{net}$  to be close to the observed value in July. The GCM overpredicts it in January.
4. Incorrect surface winds cause the simulated latent heat flux to be too large over the GS.
5. Incorrect surface winds cause the simulated sensible heat flux (SH) to be too large in the GS and the Beaufort Sea in January. The warm bias of the GCM in July causes the SH flux to have both sign and magnitude errors over the AO. The total Arctic SH flux mean was positive, although the means for the individual seas were negative. This indicates that there is a large compensating positive SH flux for land points.

6. The simulated net surface energy flux over the AO agrees with observations for January as do the individual components that comprise it. For July, however, the value is too low due to the  $LW_{net}$  and the SH flux which are both too high.
7. The simulated surface SW and LW cloud forcing are both too weak for July yielding a net which is close to the observed value
8. The simulated net SW at the top of the atmosphere is too large for July, due to the underprediction of clouds.

Comparisons for individual land locations in Section five support the above conclusions. In addition, they confirm quite clearly the GCM's problems over the Alaskan peninsula in January. The overprediction of cloud amount there lends itself to problems in the LW components and to an overprediction of precipitation.

In general, the changes needed in the CSU GCM center around the underprediction of clouds over the Arctic Ocean for July and the overprediction of clouds over land. Arctic clouds initiate a major cloud-radiation feedback mechanism (see Section 1). Thus, the errors in cloud amount have far reaching implications for the climate of the Arctic, by affecting the radiation components. We need to address two other major problems which are the warm bias of the GCM in July and the large error in surface pressures in January. Some or all of these problems may correct themselves with a more realistic ice thickness distribution which should give more realistic surface temperature, pressure and wind distributions.

# Bibliography

- Barry, M. C., J. A. Maslanik, and M. C. Serreze, The Arctic Sea Ice-Climate System: Observations and Modeling, *Rev of Geophys.*, **31**,397-422, 4 Nov. 1993.
- Barry, R. G., R. G. Crane, A. Schweiger, and J. Newell, Arctic Cloudiness in Spring from Satellite Imagery, *J Clim.*, **7**, 423-451, 1987.
- Curry, J. A., J. L. Schramm, and E. E. Ebert, Impacts of Clouds on the Surface Radiation Balance of the Arctic Ocean, *J. Met and Atmos. Phys.*, **51**, 197-217, 1993.
- Curry, J. A., and Elizabeth E. Ebert, Annual Cycle of Radiation Fluxes over the Arctic Ocean: Sensitivity to Cloud Optical Properties, *J. of Clim.*, **5**(11), 1267-1280, 1992.
- Ebert, E. A., and J. A. Curry, An Intermediate One-dimensional Thermodynamic Sea Ice Model for Investigating Ice-atmosphere Interactions, *J. Geophys. Res.*, **98**(C6), 10,085-10,109, 1993.
- Gates, W.L., AMIP: The Atmospheric Intercomparison Project, *Bull. Amer Meteor Soc.*, **73**, 1962-1970, 1992.
- Herman, G. F., and J. A. Curry, Observational and Theoretical Studies of Solar Radiation in Arctic Stratus, *J. Clim. and Applied Met.*, **23**(1), 5-24., Jan. 1984.
- Marshunova, M. S. and N. T. Chernigovskii, Radiation Regime of the Foreign Arctic, NSF-TT-72-51034, 189 pp., Natl. Sci. Found., Washington D. C., 1978.
- Maykut, G. A., Large Scale Heat Exchange and Ice Production in the Central Arctic, *J. Geophys. Res.*, **87**(C10), 7971-7984, 1982.
- Maykut, G. A., Energy Exchange Over Young Sea Ice in the Central Arctic, *J. Geophys., Res.*, **83**(C7), 3646-3658, 1978.
- Moritz, R. E., J.A. Curry, A. S. Thorndike, and N. Untersteiner, SHEBA-A research program on the Surface Heat Budget of the Arctic Ocean, Report No. 3, ARCSS OAI Science Management Office, Polar Sci. Ctr., APL-UW, Univ. of Washington, Seattle, WA., August, 1993.
- Nakamura, N., and A. H. Oort, Atmospheric Heat Budgets of the Polar Regions, *J. Geophys. Res.*, **93**(D8), 9510-9524, 1988.
- Power, Scott B., and Lawrence A. Mysak, On the Interannual Variability of Arctic Sea-Level Pressure and Sea Ice, *J. Atmos. and Oceans*, **30**(4), 551-577, 1992.
- Randall, David A., Donald A. Dazlich, and Kellyann Wittmeyer, A users guide to the Colorado State University general circulation model, Dept. of Atmospheric Sciences, Colorado State University, Fort Collins, Colorado, 1995.
- Schweiger, J. A., and J. Key, Arctic Cloudiness: Comparison of ISCCP-C2 and Nimbus-7 Satellite-derived Cloud Products with a Surface Based Cloud Climatology, *J. Clim.*, **5**(12),

TABLE 1. Comparison of standard meteorological parameters

- Schweiger, J. A., M. C. Serreze, and J. R. Key, Arctic Sea Ice Albedo: A Comparison of Two Satellite-derived Data Sets, *Geophys. Res. Lett.*, **20**(1), 41-44, 1993.
- Serreze, Mark C., Jonathon D. Kahl, and Russell C. Schnell, Low-level Temperature Inversions of the Eurasian Arctic and Comparisons with Soviet Drifting Station Data, *J. Clim.*, **5**, 615-629, June, 1992.
- Walsh, J. E., and C. M. Johnson, An analysis of Arctic Sea Ice Fluctuations, 1953-1977, *J. Phys Oceanogr.*, **9**, 580-591, 1979a.

VAR	MO	UNITS	TA	AO	OS	KBS	SRCE
wind sp	1	Ms <sup>-1</sup>	1.03	2.37	4.19	3.44	GCM
wind sp	7	Ms <sup>-1</sup>	1.33	1.74	2.32	2.72	GCM
wind sp	1	Ms <sup>-1</sup>	0.41	1.14	2.10	0.93	ECMWF
wind sp	7	Ms <sup>-1</sup>	0.97	0.18	1.09	0.72	ECMWF
mp	1	mp	1001.7	1000.8	991.8	1001.7	GCM
mp	7	mp	1010.0	1012.3	1012.9	1012.3	GCM
mp	1	mp	1014.0	1019.1	1008.8	1010.2	ECMWF
mp	7	mp	1012.9	1012.8	1011.4	1012.2	ECMWF
geop 500mb	1	m	3064.4	3021.9	3130.0	3058.7	GCM
geop 500mb	7	m	3307.9	3311.8	3332.2	3248.9	GCM
geop 500mb	1	m	3030.1	3024.4	3143.1	3010.1	ECMWF
geop 500mb	7	m	2427.4	2422.4	2419.4	2464.2	ECMWF
temp	1	K	250.02	243.92	266.07	251.80	GCM
temp	7	K	280.63	274.41	278.11	278.01	GCM
temp	1	K	248.86	240.93	267.01	258.90	ECMWF
temp	7	K	278.20	289.39	272.63	272.39	ECMWF
temp	1	K	248.70	248.70	248.70	248.70	Gen(83)
temp	7	K	274.30	274.30	274.30	274.30	Gen(83)
temp	1	K	242.70	242.70	242.70	242.70	Domini(83)
temp	7	K	272.30	272.30	272.30	272.30	Domini(83)

KEY: VAR: Variable; MO: Month; TA: Total Arctic; AO: Arctic Ocean; OS: Greenland Sea; KBS: Karasars Sea; SRCE: Source

TABLE 1. Comparison of standard meteorological parameters

VAR	MO	UNITS	TA	AO	GS	KBS	SRCE
u wind	1	Ms <sup>-1</sup>	-0.89	-1.77	-2.15	-3.34	GCM
u wind	7	Ms <sup>-1</sup>	-0.94	-1.41	-1.65	-2.24	GCM
u wind	1	Ms <sup>-1</sup>	-0.36	-1.13	-1.29	-0.92	ECMWF
u wind	7	Ms <sup>-1</sup>	-0.18	0.16	-0.61	-0.41	ECMWF
v wind	1	Ms <sup>-1</sup>	-0.53	-1.43	-3.37	0.84	GCM
v wind	7	Ms <sup>-1</sup>	-0.83	-1.02	-1.91	-1.54	GCM
v wind	1	Ms <sup>-1</sup>	-0.20	0.12	-2.82	0.17	ECMWF
v wind	7	Ms <sup>-1</sup>	-0.32	-0.01	-0.90	-0.63	ECMWF
wind sp	1	Ms <sup>-1</sup>	1.03	2.27	4.19	3.44	GCM
wind sp	7	Ms <sup>-1</sup>	1.25	1.74	2.52	2.72	GCM
wind sp	1	Ms <sup>-1</sup>	0.41	1.14	3.10	0.93	ECMWF
wind sp	7	Ms <sup>-1</sup>	0.37	0.16	1.09	0.75	ECMWF
mssl	1	mb	1001.7	1006.8	991.6	1001.7	GCM
mssl	7	mb	1010.0	1012.3	1012.9	1012.3	GCM
mssl	1	mb	1014.0	1019.1	1008.8	1010.2	ECMWF
mssl	7	mb	1012.3	1013.6	1011.4	1015.5	ECMWF
geop 500mb	1	m	5064.4	5021.3	5120.0	5026.7	GCM
geop 500mb	7	m	5567.9	5511.5	5535.2	5546.9	GCM
geop 500mb	1	m	5050.1	5024.4	5143.1	5016.1	ECMWF
geop 500mb	7	m	5457.4	5422.4	5419.4	5464.3	ECMWF
temperatre	1	K	250.05	243.95	266.07	251.86	GCM
temperatre	7	K	280.63	274.41	279.11	276.01	GCM
temperatre	1	K	248.86	240.93	267.01	258.90	ECMWF
temperatre	7	K	276.50	269.39	275.63	272.33	ECMWF
temperatre	1	K		248.70			Oort(83)
temperatre	7	K		274.30			Oort(83)
temperatre	1	K		243.70			Doronin(63)
temperatre	7	K		272.50			Doronin(63)

KEY: VAR: Variable, MO: Month, TA: Total Arctic, AO: Arctic Ocean  
 GS: Greenland Sea, KBS: Kara/Barents Seas, SRCE: Source

TABLE 2. Comparison of cloud parameters

VAR	MO	UNITS	TA	AO	GS	KBS	SRCE
low cld fr	1	Prcnt	.62	.44	.74	.53	GCM
low cld fr	7	Prcnt	.26	.15	.29	.18	GCM
low cld fr	1	Prcnt	.29	.20	.62	.59	Warren
low cld fr	7	Prcnt	.53	.64	.72	.69	Warren
low cld fr	1	Prcnt		.17			Huschke(69)
low cld fr	7	Prcnt		.65			Huschke(69)
low cld fr	1	Prcnt		.05			C-matrix Sat data
low cld fr	7	Prcnt		.12			C-matrix Sat data
mid cld fr	1	Prcnt	.38	.25	.54	.32	GCM
mid cld fr	7	Prcnt	.35	.14	.23	.20	GCM
mid cld fr	1	Prcnt	.34	.26	.46	.39	Warren
mid cld fr	7	Prcnt	.35	.36	.43	.34	Warren
mid cld fr	1	Prcnt		.30			Huschke(69)
mid cld fr	7	Prcnt		.38			Huschke(69)
mid cld fr	1	Prcnt		.13			C-matrix Sat data
mid cld fr	7	Prcnt		.12			C-matrix Sat data
hi cld fr	1	Prcnt	.44	.33	.63	.31	GCM
hi cld fr	7	Prcnt	.37	.20	.25	.23	GCM
hi cld fr	1	Prcnt	.22	.20	.13	.06	Warren
hi cld fr	7	Prcnt	.22	.26	.14	.15	Warren
hi cld fr	1	Prcnt		.30			Huschke(69)
hi cld fr	7	Prcnt		.20			Huschke(69)
hi cld fr	1	Prcnt		.35			C-matrix Sat data
hi cld fr	7	Prcnt		.24			C-matrix Sat data
tot cld fr	1	Prcnt	.79	.64	.88	.70	GCM
tot cld fr	7	Prcnt	.61	.36	.51	.43	GCM
tot cld fr	1	Prcnt	.59	.54	.79	.71	Warren
tot cld fr	7	Prcnt	.75	.82	.85	.82	Warren
tot cld fr	1	Prcnt		.80			Huschke(69)
tot cld fr	7	Prcnt		.85			Huschke(69)
tot cld fr	1	Prcnt		.69			C-matrix Sat data
tot cld fr	7	Prcnt		.44			C-matrix Sat data
cld od	1		1.63	0.89	3.59	1.13	GCM
cld od	7		3.53	1.00	2.23	1.48	GCM
cld od	1			2.20			Curry,Ebert(92)
cld od	7			8.00			Curry,Ebert(92)
tot precip	1	mm/dy	1.04	0.31	3.54	0.88	GCM
tot precip	7	mm/dy	1.23	0.20	0.74	0.39	GCM
tot precip	1	mm/dy	1.13	0.35	3.28	1.03	NCAR
tot precip	7	mm/dy	1.38	0.97	1.26	1.27	NCAR
tot precip	1	mm/dy		0.81			Vowinckel,Orvig(70)
tot precip	7	mm/dy		0.93			Vowinckel,Orvig(70)
spec humid	1	g/kg	0.50	0.25	0.90	0.61	GCM
spec humid	7	g/kg	3.74	3.12	3.86	3.33	GCM
spec humid	1	g/kg		0.40			Oort(83)
spec humid	7	g/kg		3.60			Oort(83)

TABLE 3. Comparison of radiation parameters

VAR	MO	UNITS	TA	AO	GS	KBS	SRCE
albedo	1	Prcnt	40.47	42.90	41.52	40.51	GCM
albedo	7	Prcnt	31.14	58.19	21.94	40.34	GCM
albedo	1	Prcnt		83.0			Curry,Ebert(92)
albedo	7	Prcnt		48.0			Curry,Ebert(92)
albedo	7	Prcnt		31.0			Doronin(63)
net sw	7	Wm <sup>-2</sup>	154.95	132.36	201.43	166.86	GCM
net sw	7	Wm <sup>-2</sup>		135.0			Curry,Ebert(92)
net sw	7	Wm <sup>-2</sup>		90.0			Maykut(82)
net sw	7	Wm <sup>-2</sup>		110.0			Maykut(86)
net sw	7	Wm <sup>-2</sup>		125.0			Marshunova(61)
downwrld lw	1	Wm <sup>-2</sup>	175.60	146.29	241.61	173.77	GCM
downwrld lw	7	Wm <sup>-2</sup>	288.87	243.53	273.41	256.75	GCM
downwrld lw	1	Wm <sup>-2</sup>		171.0			Curry,Ebert(92)
downwrld lw	7	Wm <sup>-2</sup>		291.0			Curry,Ebert(92)
downwrld lw	1	Wm <sup>-2</sup>		170.0			Maykut(86)
downwrld lw	7	Wm <sup>-2</sup>		310.0			Maykut(86)
downwrld lw	1	Wm <sup>-2</sup>		162.0			Marshunova(61)
downwrld lw	7	Wm <sup>-2</sup>		298.0			Marshunova(61)
net lw	1	Wm <sup>-2</sup>	46.24	48.86	50.86	55.56	GCM
net lw	7	Wm <sup>-2</sup>	58.02	68.64	62.18	63.84	GCM
net lw	1	Wm <sup>-2</sup>		20.0			Makshtas(84)
net lw	1	Wm <sup>-2</sup>		30.0			Maykut(78)
net lw	7	Wm <sup>-2</sup>		12.0			Maykut(78)
net lw	7	Wm <sup>-2</sup>		5.0			Maykut(82)
sens hf	1	Wm <sup>-2</sup>	-10.03	-11.24	23.54	7.51	GCM
sens hf	7	Wm <sup>-2</sup>	6.16	-11.89	-12.31	-9.73	GCM
sens hf	1	Wm <sup>-2</sup>			11.5		AIDJEX ob
sens hf	7	Wm <sup>-2</sup>			-5.04		AIDJEX ob
sens hf	1	Wm <sup>-2</sup>		-5.0			Levitt et al(78)
sens hf	1	Wm <sup>-2</sup>		-8.0			Makshtas(84)
sens hf	1	Wm <sup>-2</sup>		-17.0			Maykut(78)
sens hf	1	Wm <sup>-2</sup>		-11.0			Maykut(82)
sens hf	1	Wm <sup>-2</sup>		-18.0			Doronin(63)
sens hf	1	Wm <sup>-2</sup>		-11.0			Badgley(66)
sens hf	7	Wm <sup>-2</sup>		2.0			Levitt et al(78)
sens hf	7	Wm <sup>-2</sup>		5.0			Maykut(82)
sens hf	7	Wm <sup>-2</sup>		5.0			Doronin(63)
sens hf	7	Wm <sup>-2</sup>		1.0			Badgley(66)
latent hf	1	Wm <sup>-2</sup>	8.75	0.00	55.40	17.50	GCM
latent hf	7	Wm <sup>-2</sup>	32.10	5.83	23.30	11.66	GCM
latent hf	1	Wm <sup>-2</sup>			0.56		AIDJEX ob
latent hf	7	Wm <sup>-2</sup>			10.3		AIDJEX ob
latent hf	1	Wm <sup>-2</sup>		1.0			Levitt et al(78)
latent hf	1	Wm <sup>-2</sup>		2.0			Makshtas(84)
latent hf	1	Wm <sup>-2</sup>		0.0			Badgley(66)
latent hf	7	Wm <sup>-2</sup>		3.0			Levitt et al(78)
latent hf	7	Wm <sup>-2</sup>		10.0			Maykut(82)
latent hf	7	Wm <sup>-2</sup>		10.0			Doronin(63)
latent hf	7	Wm <sup>-2</sup>		5.0			Badgley(66)

TABLE 3 continued

VAR	MO	UNITS	TA	AO	GS	KBS	SRCE
net dn hf	1	Wm <sup>-2</sup>	-43.91	-38.40	-127.00	-81.62	GCM
net dn hf	7	Wm <sup>-2</sup>	57.67	70.25	129.04	102.19	GCM
net dn hf	1	Wm <sup>-2</sup>			-30.5		AIDJEX ob
net dn hf	7	Wm <sup>-2</sup>			88.4		AIDJEX ob
net dn hf	1	Wm <sup>-2</sup>		-21.0			Curry,Ebert(92)
net dn hf	7	Wm <sup>-2</sup>		95.0			Curry,Ebert(92)
net dn hf	1	Wm <sup>-2</sup>		-50.0			Maykut(78)
net dn hf	1	Wm <sup>-2</sup>		-40.0			Maykut(82)
net dn hf	7	Wm <sup>-2</sup>		100.0			Maykut(82)
sw cld for	7	Wm <sup>-2</sup>	-88.12	-21.97	-72.58	-44.94	GCM
sw cld for	7	Wm <sup>-2</sup>		-100.0			Curry,Ebert(92)
lw cld for	1	Wm <sup>-2</sup>	35.59	24.91	53.04	32.99	GCM
lw cld for	7	Wm <sup>-2</sup>	30.09	13.56	26.32	17.13	GCM
lw cld for	1	Wm <sup>-2</sup>		41.0			Curry,Ebert(92)
lw cld for	7	Wm <sup>-2</sup>		80.0			Curry,Ebert(92)
tot cl for	1	Wm <sup>-2</sup>	33.79	24.91	50.58	32.97	GCM
tot cl for	7	Wm <sup>-2</sup>	-58.03	-8.41	-46.27	-27.80	GCM
tot cl for	1	Wm <sup>-2</sup>		41.0			Curry,Ebert(92)
tot cl for	7	Wm <sup>-2</sup>		-20.0			Curry,Ebert(92)
net sw top	7	Wm <sup>-2</sup>	281.89	242.67	315.51	279.13	GCM
out lw top	1	Wm <sup>-2</sup>	158.45	153.18	167.19	160.89	GCM
out lw top	7	Wm <sup>-2</sup>	225.30	227.27	227.46	227.48	GCM
pl albedo	7	Prcnt	37.89	48.18	30.23	39.34	GCM
clr net lw	1	Wm <sup>-2</sup>	81.83	73.77	103.90	88.55	GCM
clr net lw	7	Wm <sup>-2</sup>	88.11	82.20	88.49	80.98	GCM
clr net sw	7	Wm <sup>-2</sup>	243.07	154.33	274.01	211.80	GCM

KEY: VAR: Variable, MO: Month, TA: Total Arctic, AO: Arctic Ocean  
 GS: Greenland Sea, KBS: Kara/Barents Seas, SRCE: Source

TABLE 4. Comparison of five Arctic regions

VAR	MO	UNITS	BFRT	GLND	N/B	LAP	N of 70	SOURCE
net sw top	7	Wm <sup>-2</sup>	255.94	250.54	283.47	261.44	250.89	GCM
net sw top	7	Wm <sup>-2</sup>					210.00	compiled obs
out lw top	1	Wm <sup>-2</sup>	155.80	153.68	159.97	149.72	153.59	GCM
out lw top	7	Wm <sup>-2</sup>	226.33	216.92	229.55	225.89	224.71	GCM
out lw top	1	Wm <sup>-2</sup>					160.00	compiled obs
out lw top	7	Wm <sup>-2</sup>					210.00	compiled obs
pl albedo	7	Prcnt	44.56	45.71	38.53	43.34	46.35	GCM
pl albedo	7	Prcnt					50.00	compiled obs
tot cld fr	1	Prcnt	.77	.81	.74	.62	.69	GCM
tot cld fr	7	Prcnt	.48	.65	.43	.51	.46	GCM
tot cld fr	1	Prcnt	.42	.55	.50	.48		compiled obs
tot cld fr	7	Prcnt	.62	.79	.81	.83		compiled obs
sens hf	1	Wm <sup>-2</sup>	-16.36	-21.91	3.44	-12.28	-13.67	GCM
sens hf	7	Wm <sup>-2</sup>	-8.91	-12.56	-1.91	5.09	-10.13	GCM
sens hf	1	Wm <sup>-2</sup>	-12.00					Maykut(82)
sens hf	7	Wm <sup>-2</sup>	-5.00					Maykut(82)
latent hf	1	Wm <sup>-2</sup>	0.00	2.91	20.40	0.00	2.91	GCM
latent hf	7	Wm <sup>-2</sup>	17.50	20.40	20.40	20.40	14.60	GCM
latent hf	1	Wm <sup>-2</sup>	1.00					Maykut(82)
latent hf	7	Wm <sup>-2</sup>	12.00					Maykut(82)
net dn hf	1	Wm <sup>-2</sup>	-25.19	-23.92	-76.78	-39.43	-38.09	GCM
net dn hf	7	Wm <sup>-2</sup>	65.70	53.85	81.85	49.69	64.63	GCM
net dn hf	1	Wm <sup>-2</sup>					-50.00	compiled obs
net dn hf	7	Wm <sup>-2</sup>					75.00	compiled obs
net dn hf	1	Wm <sup>-2</sup>	-35.00					Maykut(82)
net dn hf	7	Wm <sup>-2</sup>	85.00					Maykut(82)
rel humid	1	Prcnt	79.32	80.76	78.77	75.64	78.35	GCM
rel humid	7	Prcnt	77.60	69.48	72.47	82.54	78.11	GCM
rel humid	7	Prcnt					64.00	Doronin(63)

KEY: BFRT: Beaufort Sea, GLND: Greenland Sea, N/B: Norwegian/Barents Seas, LAP: Laptev Sea

TABLE 5. Comparisons for individual land locations defined in Figure 2.

ALBEDO JULY:

PLACE	GCM	MC RAD
Sodankyla	.08	.2
Jokioynen	.08	.2
Resolute	.51	2

CLEAR SKY NET LW JAN ( $Wm^{-2}$ ):

PLACE	GCM	MC RAD
Isfjord	77	70
Tromso	87	73
Karasjok	88	70
Bude	85	73
Kiruna	84	70
Sodankyla	81	70
Jokioynen	87	75
Reykjavik	119	73
Alert	63	55
Resolute	75	53
Inuvik	73	58
Barrow	80	64
Fairbanks	97	66

CLEAR SKY NET LW JULY ( $Wm^{-2}$ ):

PLACE	GCM	MC RAD
Isfjord	85	69
Tromso	93	70
Karasjok	90	69
Bude	95	69
Kiruna	91	70
Sodankyla	89	73
Jokioynen	84	70
Reykjavik	91	70
Alert	97	67
Resolute	88	66
Inuvik	65	72
Barrow	89	67
Fairbanks	95	75

DOWNWARD LW JAN ( $Wm^{-2}$ ):

PLACE	GCM	MC RAD
Isfjord	161	225
Tromso	219	264
Karasjok	203	214
Bude	220	276
Kiruna	209	214
Sodankyla	199	230
Jokioynen	215	251
Reykjavik	275	281
Alert	130	155
Resolute	156	152
Inuvik	195	159
Barrow	192	170
Fairbanks	220	178

DOWNWARD LW JULY ( $Wm^{-2}$ ):

PLACE	GCM	MC RAD
Isfjord	240	326
Tromso	324	355
Karasjok	325	364
Bude	324	364
Kiruna	332	372
Sodankyla	336	387
Jokioynen	352	380
Reykjavik	285	351
Alert	261	306
Resolute	261	312
Inuvik	265	370
Barrow	314	314
Fairbanks	314	389

NET FLUX JAN ( $Wm^{-2}$ ):

PLACE	GCM	MC RAD
Sodankyla	-22.07	-13.0
Jokioynen	-22.35	-25.0
Resolute	-22.27	-33.0

NET FLUX JULY ( $Wm^{-2}$ ):

PLACE	GCM	MC RAD
Sodankyla	18.4	100.0
Jokioynen	10.3	106.0
Resolute	64.3	141.0

NET LW JAN ( $Wm^{-2}$ ):

PLACE	GCM	MC RAD
Isfjord	57	37
Tromso	44	36
Karasjok	53	37
Bude	47	34
Kiruna	41	36
Sodankyla	41	34
Jokioynen	48	36
Reykjavik	54	36
Alert	44	37
Resolute	46	37
Inuvik	39	39
Barrow	37	42
Fairbanks	37	41

TABLE 5 continued

NET LW JULY ( $Wm^{-2}$ ):

PLACE	GCM	MC RAD
Isfjord	73	23
Tromso	45	34
Karasjok	46	31
Bude	57	31
Kiruna	56	36
Sodankyla	53	34
Jokioynen	52	39
Reykjavik	58	36
Alert	53	33
Resolute	61	27
Inuvik	46	31
Barrow	34	23
Fairbanks	45	30

NET SW JULY ( $Wm^{-2}$ ):

PLACE	GCM	MC RAD
Isfjord	158	155
Tromso	133	169
Karasjok	131	167
Bude	145	173
Kiruna	162	173
Sodankyla	160	212
Jokioynen	170	219
Reykjavik	231	196
Resolute	131	220
Inuvik	113	206
Fort Simpson	168	228
Barrow	113	211
Fairbanks	125	222

TOTAL CLOUD PERCENT JAN ( $Wm^{-2}$ ):

PLACE	GCM	MC RAD
Isfjord	63	61
Tromso	88	71
Karasjok	74	66
Bude	78	72
Kiruna	86	66
Sodankyla	84	74
Jokioynen	75	76
Reykjavik	91	68
Myugbukhta	91	42
Medvezhiv	90	77
Eureka	81	34
Resolute	77	40
Inuvik	79	53
Fort Simpson	83	56
Barrow	83	55
Fairbanks	93	62

TOTAL CLOUD PERCENT JULY ( $Wm^{-2}$ ):

PLACE	GCM	MC RAD
Isfjord	28	81
Tromso	79	71
Karasjok	81	70
Bude	77	75
Kiruna	77	69
Sodankyla	75	71
Jokioynen	66	60
Reykjavik	57	73
Myugbukhta	54	58
Medvezhiv	42	85
Eureka	98	65
Resolute	56	74
Inuvik	67	71
Fort Simpson	85	61
Barrow	85	82
Fairbanks	86	76